Ancient teeth, phenetic affinities, and African hominins: Another look at where *Homo naledi* fits in

Joel D. Irish[a,b,*], Shara E. Bailey[c], Debbie Guatelli-Steinberg[d], Lucas K. Delezene[b,e], Lee R. Berger[b]

[a] *Research Centre in Evolutionary Anthropology and Palaeoecology, School of Natural Sciences and Psychology, Liverpool John Moores University, Liverpool L3 3AF UK*
[b] *Evolutionary Studies Institute and Centre for Excellence in PaleoSciences, University of the Witwatersrand, Private Bag 3, WITS 2050, Johannesburg, South Africa*
[c] *Department of Anthropology, New York University, New York, NY 10003, USA*
[d] *Department of Anthropology, Ohio State University, Columbus, OH 43210, USA*
[e] *Department of Anthropology, University of Arkansas, Fayetteville, AR 72701 USA*

* Corresponding author.
E-mail address: J.D.Irish@ljmu.ac.uk (J.D. Irish).

Abstract

A new species of *Homo*, *Homo naledi*, was described in 2015 based on the hominin skeletal remains from the Dinaledi Chamber of the Rising Star cave system, South Africa. Subsequent craniodental comparative analyses, both phenetic and cladistic, served to support its taxonomic distinctiveness. Here we provide a new quantitative analysis, where up to 78 nonmetric crown and root traits of the permanent dentition were compared among samples of *H. naledi* (including remains from the recently discovered Lesedi Chamber) and eight other species from Africa: *Australopithecus afarensis*, *Australopithecus africanus*, *Paranthropus boisei*, *Paranthropus robustus*, *Homo habilis*, *Homo erectus*, Middle Pleistocene *Homo* sp., and Pleistocene and Holocene *Homo sapiens*. By using the mean measure of divergence distance statistic, phenetic affinities were calculated among samples to evaluate interspecific relatedness. The objective was to compare the results with those previously obtained, to assess further the taxonomic validity of the Rising Star hominin species. In accordance with

earlier findings, *H. naledi* appears most similar dentally to the other African *Homo* samples. However, the former species is characterized by its retention and full expression of features relating to the main cusps, as well as the root numbers, with a near absence of accessory traits—including many that, based on various cladistic studies, are plesiomorphic in both extinct and extant African hominins. As such, the present findings provide additional support for the taxonomic validity of *H. naledi* as a distinct species of *Homo*.

Introduction

Where does *Homo naledi* fit in relative to other hominins? In the taxonomic

description of the skeletal and dental remains, Berger et al. (2015) found what they

considered to be enough similarities with *Homo habilis, Homo rudolfensis, Homo erectus,*

and *Homo heidelbergensis* to assign the new fossils to the genus *Homo*, yet enough

distinctions to merit a separate species. As would be expected, academic discussion

concerning the "validity of *H. naledi* as a new and distinct species" ensued (Randolph-

Quinney, 2015a:2; Von Mirbach, 2015; Schwartz, 2015; among other issues, e.g., Val, 2016),

with one researcher even suggesting that an assignment to the genus *Australopithecus* may be

more appropriate (see the discussion in Randolph-Quinney, 2015a:2). Of course, at that time

1) a phylogenetic analysis had yet to be conducted (see also Randolph-Quinney, 2015b), 2)

remains from the Lesedi Chamber of the Rising Star cave system, whose morphology

supports the original taxonomic description, had not been found (Hawks et al., 2017), and 3)

the date of the specimens of *H. naledi* from the Dinaledi Chamber (Berger et al., 2015), ca.

335–236 ka, was unknown (Dirks et al., 2017).

In a quantitative study based on published cranial data, Thackeray (2015) agreed that

a distinct species status within the genus *Homo* is justified. Of his 11 African comparative

samples, *H. naledi* appears most similar to *H. habilis* and, to a lesser degree, *H. rudolfensis*

and *H. erectus*. These findings are based on a phenetic method (Thackeray, 2007) that yields

standard errors of m-coefficients from pairwise comparisons of specimens in regression

equations. This methodological approach is not without criticism, since the results are said to

be dependent on variable number, among other issues (Gordon and Wood, 2013). More

recently, Dembo et al. (2016) used Bayesian phylogenetic analyses on a supermatrix of

craniodental data in *H. naledi* and 19 hominin species from Africa, Europe, and Asia. They

concurred that *H. naledi* is a separate species, in that it forms a clade with members of the

genus *Homo*, although its position relative to species within that clade is ambiguous (Dembo et al., 2016). This was an ambitious first attempt at a cladistic analysis of the newly described species using many comparative hominin samples and characters. However, as the authors themselves acknowledged, there are several methodological concerns involving the treatment of various characters and character states.

In this paper we present results of a phenetic analysis based on 78 nonmetric dental traits, to explore further how *H. naledi* may relate to other hominin species. These traits have been observed in a range of fossil hominins, but, driven largely by geographic provenience, the focus of study is *H. naledi* and other African species, like Thackeray (2015) and, for the most part, Berger et al. (2015) and Hawks et al. (2017). The extent of the skeletal assemblage from the Dinaledi Chamber (≥15 individuals; Berger et al., 2015) and Lesedi Chamber (≥3 individuals; Hawks et al., 2017) in the Rising Star cave system also influences approach. Ten samples comprising eight different species of *Australopithecus*, *Paranthropus*, and *Homo* are compared with *H. naledi*, but only eight of these with enough specimens to record the traits multiple times, at least to the extent possible, are analyzed quantitatively here (though see Supplementary Online Material [SOM] S1−-S3); the aim is to consider at least some of the substantial variation that occurs within groups (or in this case, species) relative to that between groups (e.g., Relethford, 1994, 2001; Templeton, 1999; Leigh et al., 2003).

Although a cladistic analysis of nonmetric dental data is possible, like Bailey (2002a) and Irish et al. (2013, 2014a), standard coding criteria do not adequately address character variability—see concerns of Asfaw et al. (1999) and Curnoe (2003), also below—given the major increase in trait number, as well as larger sample sizes, relative to these prior studies. Alternate strategies for coding character states are available and have been investigated (e.g., Bailey, 2002a). However, all have weaknesses (see below) to match their strengths (Thiele, 1993; Stringer et al., 1997; Wiens, 1995, 2001; Ried and Sidwell, 2002; Schols, 2004). Thus,

to best utilize the polymorphic nature of these traits, a non-phylogenetic method, the mean measure of divergence distance statistic (MMD), was applied here to trait frequencies from the nine largest samples to calculate phenetic affinities among *H. naledi* and these other African hominins (Sjøvold, 1977; Irish, 2010).

The MMD has been used before to compare dental data in Plio-Pleistocene species, as sample sizes allowed (Irish, 1998; Bailey, 2000, 2000a; Martinón-Torres et al., 2012). It is preferred over several other distance measures, including the pseudo-Mahalanobis D^2, by many researchers who study recent humans. Among several advantages, the most critical is that the MMD uses summary data rather than individual trait scores to address missing data that characterize fragmentary specimens in archaeological and, as above, paleontological, contexts (see Materials and methods). A supplementary technique, such as multidimensional scaling in this study, is then often used to visualize patterning of intersample distances. "It is all but certain that these phenotypic patterns reflect underlying genetic variation" (Rightmire, 1999:2); thus, it is assumed that phenetic similarity provides a reasonable approximation of genetic relatedness, at least based on the findings of recent human studies (e.g., Scott et al., 1983; Larsen, 1997; Scott and Turner, 1997; Martinón-Torres et al., 2007, 2012; Hughes and Townsend, 2013a, b; Rathmann et al., 2017).

In sum, the intent of this study is twofold: 1) to use the dental nonmetric data to assess interspecific relationships based on overall similarity among the 11 total African samples, and 2) compare these results with those from Thackeray (2015) and Dembo et al. (2016), based on different data and methods. The overarching objective, then, is to continue work toward an improved understanding of where and how *H. naledi* 'fits in' relative to other species of hominins.

Materials and methods

Dental trait recording

Sixty-six of the 78 nonmetric traits in this study are part of the Arizona State University Dental Anthropology System (ASUDAS), used to record tooth crown and root variability of the permanent dentition (Turner et al., 1991; Scott and Turner, 1997; Scott and Irish, 2017); the remaining 12, routinely used by the second author, S.E.B, are detailed below. Over 100 ASUDAS traits could potentially be scored in each specimen depending on completeness, but nearly a third of these were dropped from consideration straightaway because they are either universally absent or present in the Plio-Pleistocene hominins. The former category includes tricusped upper premolars, distosagittal ridge P^3, peg/reduced M^3, 2-rooted C_1, and I^2, P^4, M^3, I_1, P_4, and M_3 agenesis, among several others seen only in recent humans. The latter category includes root number M^1 (i.e., 3), groove pattern M_1 (Y), root number M_1 (2), and the lower molar metaconulids, which are 100% present in all samples. Another point considered for initial trait selection concerns the correlation of expression within a tooth class or field. For example, a Carabelli's cusp can be present on the M^1 through M^3, but it is routinely reported only on the M^1 to avoid data redundancy (Turner et al., 1991; Scott and Irish, 2017). That said, we have found that, depending on the trait(s) and sample(s), a priori deletion may not be warranted without first quantifying the strength of the correlation in trait editing (described below). The 66 ASUDAS traits, including many that can be expressed on multiple teeth, are listed below in Table 1 (see Results).

Despite concern by some (e.g., Carter et al., 2014), most traits are already routinely recorded by paleoanthropologists, particularly those relating to: 1) relative size variation and position of the main molar cusps (e.g., upper molar metacone and hypocone, lower molar hypoconulid, lower molar groove pattern), 2) accessory cusps and crown features (e.g., upper molar cusp 5, Carabelli's cusp, and parastyle, and lower molar anterior fovea, deflecting

wrinkle, protostylid, and cusp 7), 3) root number, and 4) other variants (e.g., labial curvature I[1], upper incisor shoveling, upper and lower molar enamel line extensions, Tomes' root P$_3$). The key difference is that recording of these ASUDAS traits is standardized, to generally include even the extreme expressions seen in some early hominins, with certain exceptions (Bailey, 2002a; Martinón-Torres et al., 2007, 2012; Scott and Irish, 2017) that do not concern the African species in the present study.

As detailed in the following references, beyond standardization to promote intra- and interobserver replicability, ASUDAS traits hold six advantages. First, they are recorded with the aid of stock reference plaques and guidelines to describe minimum, maximum, and a range of intermediate grades on an ordinal scale (Turner et al., 1991; Scott and Turner, 1997; Scott et al., 2016; Scott and Irish, 2017), so the points of reference are fixed among studies; to illustrate, a certain trait may be defined by grades of, say, 0–3 instead of more subjective criteria (see Asfaw et al., 1999), such as 'absent,' 'slight,' 'moderate,' and 'strong,' which can vary by observer and population (see also the discussion concerning character state code differences among studies in Dembo et al., 2016). Second, the traits, as noted, possess a high genetic component in expression, at least in recent humans, where in some studies heritability exceeds 0.8 (Scott, 1973; Larsen, 1997; Scott and Turner, 1997; Rightmire, 1999; Martinón-Torres et al., 2007; Hughes and Townsend, 2013a,b). This information parallels the statement that "paleoanthropologists consider teeth the 'safe box' of the genetic code" (Martinón-Torres et al., 2007:7); thus, beyond extraordinary exceptions where aDNA may be present in Plio-Pleistocene material, these nonmetric traits come as close as possible to genetic data (e.g., Hubbard et al., 2015; Rathmann et al., 2017; see also Leigh et al., 2013). Third, as mostly 'secondary' nonmetric features unimportant to overall tooth structure or function, at least in recent humans, these traits are thought to be minimally affected by selection (Scott and Turner, 1997; Leigh et al., 2003); so, along with the preceding point, they are more likely

to reflect biological ancestry than adaptation. Fourth, many crown structures are observable despite slight wear. Of course, to avoid biasing the data (Burnett, 2016), suitable scoring restraint must be exercised (see Nichol and Turner, 1986; Turner et al., 1991; Burnett et al., 2013; Stojanowski and Johnson, 2015), especially with near-occlusal traits affected at early wear stages (Burnett, 2016). Fifth, although polymorphic "they evolve very slowly" (Scott and Turner, 1997:13), so are ideal for biodistance analyses (Larsen, 1997) of both synchronic and diachronic samples. Sixth, the sexes can be pooled due to low or no sexual dimorphism in expression among recent humans (Scott, 1973, 1980; Smith and Shegev, 1988; Bermúdez de Castro, 1989; Turner et al., 1991; Hanihara, 1992; Irish, 1993; Scott and Irish, 2017). This, of course, cannot be verified for fossil hominins, but such a possibility is at least encouraging, given: 1) an inability to determine the sex of most Plio-Pleistocene specimens and 2) the need to maintain already-small sample sizes.

With all of this said, the ASUDAS "does not include some features that are important for characterizing some [fossil] groups," primarily in upper and lower premolars (Martinón-Torres et al., 2007:13282, 2012; also Bailey, 2002a, b; Irish and Guatelli-Steinberg, 2003). The reason, understandably, is that the system was initially conceived to record and compare recent human crown and root morphology. As such, 12 additional nonmetric traits routinely recorded by S.E.B. are included (see Bailey, 2002a, b; Bailey and Lynch, 2005; Bailey and Hublin, 2013; Table 1, traits 67–78), though establishing that their attributes are comparable to that of the ASUDAS is still a work in progress. As a result, 78 total crown and root traits were employed to describe and compare samples. This number is purposefully much larger than that used in previous dental studies of fossil hominins (Stringer et al., 1997; Irish, 1998; Bailey, 2000; Irish and Guatelli-Steinberg, 2006; Martinón-Torres et al., 2007, 2012; Irish et al., 2013), because estimates of biological distance and/or ancestry are unquestionably more powerful if based on many rather than few traits (Livingstone, 1991; see also Dembo et al.,

2016; Sjøvold, 1977). Further, all 78 have been recorded and/or at least observed in Plio-Pleistocene species around the world (Johanson et al., 1982; Wood and Abbot, 1983; Wood and Engleman, 1988; Tobias, 1991; Stringer et al., 1997; Irish, 1998; Bailey, 2002a,b, Bailey and Lynch, 2005; Bailey and Hublin, 2013; Irish and Guatelli-Steinberg, 2003; Martinón-Torres et al., 2008, 2012, 2013; Irish et al., 2013).

Lastly, because most of these traits are expressed bilaterally, it is necessary to select the antimere to study. Oftentimes, either the right or left side is scored in an individual (Green et al., 1979; Haeussler et al., 1988). Another approach, as used here, is to record the trait in both antimeres and, allowing for any possible asymmetry, count the side that has the highest expression (Turner and Scott, 1977); to maximize sample size if one antimere is missing, the existing side is counted. This is standard ASUDAS procedure (Turner et al., 1991; Scott and Turner, 1997; Scott et al., 2016; Scott and Irish, 2017), and assumes scoring for the maximum genetic potential in trait expression (Turner, 1985; Turner et al., 1991; Scott and Turner, 1997; Scott et al., 2016; Scott and Irish, 2017).

Quantitative analyses

For comparative analyses, the rank-scale dental traits had to be dichotomized into categories of present or absent, a step dictated by the multivariate nonmetric distance statistics available (Sjøvold, 1977; Konigsberg, 1990), including the MMD. This practice also streamlines the presentation of individual trait data and ameliorates further any concordance issues in scoring that remain despite standardization (Nichol and Turner, 1986; Turner et al., 1991), especially between observers (Stojanowski and Johnson, 2015). The clear downside is that the complete range of data is not presented, precluding others from dichotomizing them differently. So, a list of traits with alternate breakpoints can be made available upon request.

In prior studies, dichotomization has been based on each particular trait's appraised morphological threshold (Haeussler et al., 1988) in recent world populations as determined by Scott (1973), Nichol (1990), and others, using standard procedure (Turner, 1987). Thus, the present/absent breakpoints are consistent across studies, although some may be altered if necessary. For example, cusp 7 M_1 is common enough in sub-Saharan Africans (see Irish, 1997) that a grade of 2+ is considered 'present' in analyses of them to better differentiate among samples, contra 1+ when comparing other groups (cf. Scott and Turner, 1997). Given the extreme expression of some dental traits in fossil hominins, most breakpoints were raised systematically to better identify interspecific variation; several emulate those of Martinón-Torres et al. (2012) in their Sima de los Huesos study (see trait dichotomies in Table 1). Some examples include: labial curvature I^1 (i.e., raised from grade 2 and above, to 3+), upper incisor tuberculum dentale (2+ to 3+), metacone M^1 (4+ to 5), upper molar cusp 5 (2+ to 3+), cusp number M_3 (6 to 7), lower molar protostylid (1+ to 4+), and Tomes' root P_3 (3+ to 5). A few breakpoints were increased to an even greater extent to target early hominin variation, such as lingual cusp P_4 (from 2+ to 8+) to capture any indication of molarization. Beyond addressing the greater expression, these increases can further enhance sample sizes (Burnett, 2016) because certain traits on worn teeth are often still discernable at higher grades. One breakpoint was lowered, upper/lower molar enamel extension (2+ to 1), to specifically account for a slight projection of the buccal enamel line between roots seen in some fossil molars (e.g., Johanson et al., 1982). Breakpoints for the 12 non-ASUDAS traits were set by S.E.B. (Bailey, 2002a, b; Bailey and Lynch, 2005; Bailey and Hublin, 2013) to mostly record absence (grade 0) vs. presence (any visible expression, i.e., 1+) in several cases to minimize observer error. More information about dichotomizing threshold traits, including rationale, strategies, and standard breakpoints for comparison to the present values, are presented in Scott and Turner (1997) and elsewhere (Scott et al., 2016; Scott and Irish, 2017).

The dichotomized data from samples of sufficient size (see below) were submitted to the mean measure of divergence (MMD) statistic to calculate interspecific phenetic affinities (Sjøvold, 1977; Irish, 2010). The MMD yields numeric distances between sample pairs, where smaller values indicate more similitude and vice versa. To find out whether two samples differ significantly the distance is compared with its standard deviation, so if the MMD>2×s, the null hypothesis $P_1 = P_2$ (where P = population sample) is rejected at the 0.025 alpha level (Sjøvold, 1977). The formula used here contains the Freeman and Tukey angular transformation to correct for low or high frequencies of traits and, importantly, small sample sizes (Sjøvold, 1973, 1977; Green and Suchey, 1976; Irish, 2010). As mentioned, the MMD is additionally well suited for comparing small samples because it uses summary data, meaning that all specimens can be included irrespective of individual completeness. Other nonmetric distance statistics require input of individual cases that, when excessively affected by missing data, necessitate pairwise or list-wise deletion. The deletion of numerous variables will obviously moderate results. Deletion of cases, beyond reducing the already-small sample sizes, can also bias results because the few complete cases that remain are not likely to be representative of the overall sample (Little and Rubin, 2014).

Although it is a robust statistic (Irish, 2010), the MMD has several assumptions concerning problematic data (Harris and Sjøvold, 2004). For example, though using summary data, it is assumed that traits with an excessive number of missing observations are not used because the bias transformation was not originally designed to correct for samples of $n < 10$ (Green and Suchey, 1976; Green et al., 1979). The same goes for fixed or largely invariant traits across samples, despite the use of the same bias transformation that corrects for low (≤0.05) or high (≥0.95) frequencies; such traits provide little useful information to detect intersample variation and can yield negative MMD distances—a statistical artifact that has "no biological meaning" (Harris and Sjøvold, 2004:91). And, while recommended that as

many traits as possible be used to compare samples, they should not be highly intercorrelated, otherwise differential weighting of the underlying dimensions may produce inaccurate distances (Sjøvold, 1977). Therefore, following standard editing procedure (Irish, 2005, 2006, 2010, 2016), all fixed or predominantly invariant traits across hominin samples were first detected qualitatively for deletion. Additional traits that are minimally discriminatory were identified by submitting their percentages of occurrence to principal components analysis (PCA); those having what are considered low component loadings, < □0.5□, were dropped (Abdi and Williams, 2010). Then, the Kendall's tau-*b* rank correlation coefficient was used to determine which trait pairs are strongly correlated, i.e., $\tau_b \geq |0.5|$ (see Cohen, 1988), in a final round of deletion.

Lastly, once calculated, the MMD matrix was submitted to multidimensional scaling (MDS) to illustrate intersample affinities. Interval-level MDS (IBM SPSS 24.0 Procedure Alscal) was applied because the range of distance values emulates continuous data. In the process, the sum of squared differences between Euclidean values from the distance matrix (d_{ij}) and those in the resulting ($d\,\hat{}_{ij}$) matrix are minimized, or optimally scaled (Hintze, 2007).

Three-dimensional plots illustrate the present relationships. Though seemingly less intuitive because additional interpretation is required, assessing affinities with MDS is less subjective (Kruskal and Wish, 1978; Cox and Cox, 1994; Borg and Groenen, 1997) than what are essentially one-dimensional tree diagrams; dendrograms, for example, more or less force samples into groups and often return alternate results depending upon which hierarchical clustering algorithm is used (Romesburg, 1984).

Studied sample

The original sample of *H. naledi* consists of 122 dental specimens from site UW 101 in the Dinaledi Chamber (Berger et al., 2015). To maximize the sample size, six specimens

attributed to this species from site UW 102 in the Lesedi Chamber were included (see below),
though the date of this material is not yet substantiated (Hawks et al., 2017). Nonmetric traits
were also directly recorded or, in some instances, derived from published data (below) in the
10 other African samples noted in the Introduction. Eight consist of Plio-Pleistocene species:
A. afarensis (*n* = 64 individual specimen numbers), *A. africanus,* (*n* = 138), *P. boisei* (*n* =
37), *P. robustus* (*n* = 166), *H. habilis* (*n* = 19), *H. erectus* (*n* = 50), Middle Pleistocene *Homo*
(*n* = 13)—also attributed to *H. heidelbergensis, Homo rhodesiensis,* and 'archaic *H. sapiens*'
(see Berger et al., 2015), and Middle to Late Pleistocene *H. sapiens* (*n* = 38). The other two
samples consist of Holocene age *H. sapiens* from South (*n* = 305 individuals) and East (*n* =
174) Africa.

The first six comparative fossil species were chosen because they represent the three
main, later hominin genera and, most importantly (as above), are represented by enough
individuals to permit at least some indication of intraspecific variation for the interspecific
comparisons. Although few in number, the *H. habilis* data were not supplemented. That is,
traits recorded in eight *H. rudolfensis* specimens could potentially be included (i.e., as *H.*
habilis sensu lato), but these add too little data to those in the most need of augmentation,
maxillary anterior tooth traits (refer to Table 1), to justify the pooling of different species
with demonstrably distinct dental features. Therefore, all pairwise MMD affinities with the
smallest of these six samples should be interpreted with extra caution. The even fewer
maxillary anterior teeth of African *H. erectus* did, however, necessitate sample augmentation,
in this case with what is said to be *H. ergaster* (or at least a close relative of similar age) from
Dmanisi (Rightmire et al., 2006; Baab, 2008; Martinón-Torres et al., 2008; Martinón-Torres,
personal communication, 2016; Rightmire and Lordkipanidze, 2010; Lordkipanidze et al.,
2013), and three maxillary incisors and one canine from African *Homo* sp. (Moggi-Cecchi et
al., 2006; Curnoe, 2010; Moggi-Cecchi et al., 2010; Berger et al., 2015; specimen numbers

listed below). This pooling of specimens, especially African *Homo* sp. (albeit just four teeth) is not ideal, but was effected out of methodological concern to increase power of the MMD. It facilitates comparisons of *H. naledi* with the optimal regional representation of later Plio-Pleistocene *Homo* for the present analyses, without requiring the inclusion of geographically disparate Asian *H. erectus*.

Other African hominin species to which it could be of use to compare *H. naledi,* like in the aforementioned studies (Berger et al., 2015; Thackeray, 2015; Dembo et al., 2016; Hawks et al., 2017), are not of sufficient sample size for the present quantitative approach, including: *Australopithecus anamensis, Australopithecus garhi, Australopithecus sediba, Paranthropus aethiopicus, Kenyanthropus platyops,* and *Homo rudolfensis.* The remaining two comparative samples in this study are similarly affected: African Middle Pleistocene *Homo* and Middle/ Late Pleistocene *H. sapiens*. These small, heterogeneous samples are included because of some age overlap with *H. naledi*, ca. 700–130 ka and ca. 315-60 ka, respectively (Geraads et al., 1986; Grine, 2000; Oujaa et al., 2017; Richter et al., 2017), though just eight specimens from Florisbad, Hoedjiespunt, and Jebel Irhoud (see below) actually date between 335–236 ka (Dirks et al., 2017). Comparable non-African data are largely unavailable to supplement the Middle Pleistocene *Homo* sample, with exceptions (Martinón-Torres et al., 2012; and below) and, as stated, alternative samples of African *Homo sapiens* are used in this study. As such, in this paper the analyses of these two fossil comparative samples focus on qualitative assessments of trait percentages.

The final two of 10 comparative samples comprise more recent *H. sapiens* from the two principal African geographic regions in which hominin remains have been recovered. The first includes Early through Late Holocene (ca. 12,000–2,000 BP) South African (SA) crania from Fish Hoek, Matjes River, Knynsa, Oakhurst Rockshelter, and other sites (Irish et al., 2014b). The second sample consists of Early to Late Holocene (ca. 10,000–1,500 BP)

East African (EA) crania from Kenya and Tanzania that are also derived from various sites: Bromhead's site, Gambles Cave, Homa, Hyrax Hill, Kanam, Kisima, Koobi Fora, Loboi, Lowasera, Lothagam, Makalia, Molo, Naivasha, Nakuru, Ngorongoro, Njoro, and Willey's Kopje (J.D.I., unpublished data). They represent the oldest South and East African *H. sapiens* samples assembled by J.D.I., and are thought to be direct descendants of considerably older autochthonous populations in the regions (Leakey, 1935; Robbins et al., 1980; Morris, 2002, 2003; Stynder et al., 2007).

All 479 dentitions of the Holocene *H. sapiens* were observed by J.D.I. The following 526 Plio-Pleistocene specimens, for which dental data were recorded, were observed by the first three authors.

Australopithecus afarensis AL 128-23, 145-35, 176-35, 188-1, 198, 199-1, 200-1a, 200-1b, 207-13, 241-14, 266, 277-1, 288-1, 311-1, 315-22, 330-5, 333-1, 333-2, 333-82, 333-90, 333-103, 333w-1, 333w-46, 333w-57, 333w-58, 333w-60, 333x-2, 333x-3, 333x-4, 333x-20, 366-6, 400-1a, 400-1b, 411-1, 413-1, 417-1a, 417-1d, 438-2, 440-1, 486-1, 620-1, 655-1, 763-1, 996-1; EP 162/00; Garusi 1; LH 1, 2, 3d, 3f, 3g, 3n, 3p, 3r, 3s, 3t, 4, 6c, 14i,j,g, 14f&e, 17, 24, 25; and Maka 12/1.

Australopithecus africanus MLD 2, 6, 18, 19, 27, 28, 44, 45; STS 1, 4, 5, 7, 8, 9, 12, 17, 18, 22, 23, 24, 30, 35, 37, 38, 41, 43, 46, 47, 50, 52, 53, 55, 55B, 56, 57, 59, 61, 62, 71; STW 1, 6, 13, 14, 15, 18, 20, 43, 59, 61, 73, 106, 107, 109, 110, 111, 123, 126, 127, 128, 131, 132, 133, 142, 169, 179, 183, 189, 192, 196, 202, 204, 213, 222, 230, 231, 233, 234, 235, 237, 241, 246, 252, 280, 285, 306, 308, 309, 312, 327B, 327C, 327D, 353, 369, 379, 384B, 384C, 384D, 384E, 402, 404, 410, 412, 413, 414, 415, 425, 429, 430, 446, 450, 491, 498A, 498B, 498C, 498D, 502, 524, 529, 536, 537, 555, 560C, 560D, 560E, 586; Taung; and TM 1511, 1512, 1519, 1520, 1523, 1527, 1528, 1531, 1534, 1561. Lockwood and Tobias (2002) suggested that STW 183 (above) also shows similarities to *P. robustus* and *Homo* sp.

Paranthropus boisei KNM-CH 1; KNM-ER 403, 404, 729, 733, 801, 802, 810, 816, 818, 1171, 1467, 1477, 1509, 1804, 1816, 1818, 1819, 1820, 3229, 3230, 3737, 3885, 3886, 3890, 3952, 6082, 6128, 15930, 15940, 15950, 17760; KNM-WT 17396, 17400, 18600, 25520; and OH 30.

Paranthropus robustus DNH 1, 8, 10, 12, 14, 15A-B, 16, 17, 18, 19, 21, 22, 26, 27, 28, 29, 34, 40, 41, 46, 51, 53, 54, 57B, 60, 68, 74, 75, 79A,, 81; KB 5063, 5222, 5223, 5383; TM 1517, 1536, 1600, 1601, 1603; SK 1, 2, 3, 5, 6, 7, 9, 11, 12, 13, 14, 16, 17, 19, 23, 24, 25, 28, 29, 30, 31, 32, 33, 34, 37, 39, 41, 42, 44, 46, 47, 48, 49, 52, 55, 55B, 57, 61, 62, 63, 65, 65A, 67, 69, 70, 71, 72, 73, 74, 74A, 75, 79, 81, 83A, 83B, 85, 86, 88, 93, 98, 99, 100, 883, 885, 891, 1512, 1586, 1587, 1588, 1589, 1591, 1593, 1595, 2354, 3114, 3300, 3971, 3974, 3975, 3976, 6934, 14001, 14003, 14030, 14129, 14246, 14251, 24660, 24661, 27524; SKX 240, 242, 265, 268, 271, 1016, 1313, 1788, 3354, 3355, 3356, 3601, 4446, 5002, 5004B, 5007, 5013, 5014, 5023, 6013, 10643, 19031, 20078, 25296, 26967, 28724, 32162, 37663, 42207, 50079; and SKW 5, 4767, 4772. Braga and Thackeray (2003) suggested that KB 5223 (above) may belong to *Homo* sp.

Homo habilis KNM-ER 1501, 1502, 1805, 1813, 1814, 42703; and OH 4, 6, 7, 13, 15, 16, 21, 24, 27, 39, 44, 45, 62.

Homo erectus KNM-BK 67, 8518; KNM-ER 730A, 731, 803H-I, 806B-C, 807A-C, 808A-G, 809A, 817, 820, 992A-C, 1462, 1480, 1506A-B, 1507, 1508, 1808G-H, 1812A,C, 3733; KNM-WT 15000, 37745, 38340; OH 12, 22, 51; SK 15, 18a, 27, 45, 847, 2635; SKW 3114; SKX 268, 2354, 2355, 2356; and D 211, 2677, 2700, 2732, 2735, 2736, 2882, 3672, 3698; the latter nine Dmanisi specimens, attributable to *H. ergaster* or a closely related species, were included to increase sample size. Curnoe (2010) suggested that SK 15, 27, 45, and SKW 3114 (above) belong to *Homo gautengensis*.

Homo sp. DNH 45, 71; KNM-BK 14297; and SE 1937. These African *Homo* specimens with indeterminate species assignment were included with *H. erectus* (above) to increase sample size.

Middle Pleistocene *Homo* Cave of Hearths; Florisbad 1; Herto (BOU-VP-16/1); Hoedjiespunt (HDP1-1, HDP1-2); Kabwe 1; Sidi Abderrahmane; Rabat-Kébibat; Thomas Quarry I (94 OA 23-24, 95 SA 26 # 89, 95/96 SA 26 # 88, 2006 PA 24 # 107); Tighenif (1, 2).

Homo naledi UW 101 001, 005, 006, 010, 020, 037, 038, 039, 073, 144, 145, 182, 184, 277, 284, 285, 297, 298, 333, 334, 335, 337, 339, 344, 347, 358, 359, 361, 377, 383, 412, 417, 418, 445, 455 , 501, 505, 506, 507, 516, 525, 527, 528, 544, 582, 583, 589, 591, 593, 594, 601, 602, 706, 708, 709, 729, 786, 789, 796, 800, 808, 809, 814, 816, 850, 867, 886, 887, 889, 905, 908, 931, 932, 985, 998, 999, 1002, 1004, 1005, 1006, 1012, 1014, 1015, 1063, 1075, 1076, 1107, 1126, 1131, 1132, 1133, 1135, 1142, 1261, 1269, 1277, 1304, 1305, 1362, 1396, 1398, 1400, 1401, 1402, 1463, 1471, 1522, 1548, 1556, 1558, 1560, 1561, 1565, 1574, 1588, 1605, 1610, 1662, 1676, 1684, 1688, 1689; and UW 102 6A, 11, 16, 24, 28, 89.

Middle/Late Pleistocene *Homo sapiens* Die Kelders AP 6242, 6258, 6264, 6275, 6277, 6279, 6280, 6281, 6282; Equus Cave H1, 2, 3, 4, 5, 6, 7, 8, 9, 10, 11, 12, 71/33; Haua Fteah; Jebel Irhoud 3, 10, 11, 21, 22; Klasies River KRM 13400, 14691, 14692, 14693, 14694, 14696, 16424, 41815; Mumba XXI; Sea Harvest PQ-S2878.

All ASUDAS data in *A. africanus, P. boisei, P. robustus,* East African *H. erectus,* South African *H. erectus* and *Homo* sp., and *H. naledi* were directly recorded by J.D.I. Many ASUDAS data in *A. afarensis* and *H. habilis* were recorded by D.G.-S., although some traits in these samples subsequently chosen for inclusion in the study, i.e., within multiple members of a tooth class (above), were derived from high resolution casts and publications (Johanson et al., 1982; Tobias, 1992; Kimbel and Delezene, 2009) by J.D.I.; Dmanisi *H. ergaster* data were recorded in the same manner (in Martinón-Torres et al., 2008), as were African Middle

Pleistocene *Homo* (Tobias, 1971; Berger and Parkington, 1995; White et al., 2003; Bermúdez de Castro et al., 2007; Raynal et al., 2010; Zanolli and Mazurier, 2013; Smith et al., 2015; Oujaa et al., 2017) and Middle/Late Pleistocene *H. sapiens* (McBurney et al., 1953; Grine and Klein, 1985, 1993; Bräuer and Mehlman, 1988; Rightmire and Deacon, 1991; Grine, 2000, 2012; Smith et al., 2007; Hublin et al., 2017).

Finally, S.E.B. recorded the non-ASUDAS premolar traits in all samples except East African *H. sapiens*; the latter data were scored by J.D.I. from photographs of five specimens because they were not originally recorded. With regard to potential observer error between these authors, both recorded the same Neanderthal tooth casts independently for prior studies (Irish, 1998; Bailey, 2002a), with no significant observer differences detected in the presence and absence of dichotomized traits (i.e., χ^2, $p > 0.05$). Observer error between J.D.I. and D.G.-S. was also found to be random, non-directional, and insignificant (χ^2, $p > 0.05$) in a previous study (detailed in Irish and Guatelli-Steinberg, 2003).

Results

The percentages of specimens that express each trait and the total number scored are provided in Table 1. Small sample size typifies many traits, not only in *H. habilis* and to a lesser extent *H. erectus*, but also in others such as *P. boisei*. Of course, Middle Pleistocene *Homo* evidences the most missing data, while the Middle/Late Pleistocene *Homo sapiens* sample is comparably affected. Nevertheless, a qualitative comparison of values suggests that notable intersample variation occurs within the tooth classes (e.g., molar traits in *H. naledi* vs. *H. sapiens*) and throughout the dentition (e.g., *A. afarensis*/EA *H. sapiens*; *P. robustus*/SA *H. sapiens*). Similarities in percentages are also evident (*A. afarensis*/*A. africanus*; *P. boisei*/*P. robustus*; *H. habilis*/*H. erectus*; EA *H. sapiens*/SA *H. sapiens*).

All data, excluding Middle Pleistocene *Homo* and Middle/Late Pleistocene *Homo sapiens*, were then submitted to the MMD. However, because the statistic routinely produces

viable results even when the above-mentioned assumptions have not been met, that is, before editing (Irish, 2010; Irish et al., 2014b; Irish, 2016), it was decided to first analyze *H. naledi* and the eight remaining comparative samples using all 78 traits (77 for *P. boisei*, *H. erectus*); the goal, simply, was to obtain an initial indication of interspecific affinities. The symmetric 78-trait MMD matrix is in Table 2. The MDS solution yields excellent representation of the matrix (Borgatti, 1997), as plotted in Figure 1, with $r^2 = 0.961$ and a Kruskal's stress formula 1 of 0.088. The EA and SA *H. sapiens* are not significantly different from each other (MMD $= 0.005, p \geq 0.025$). Several other sample pairs also do not differ significantly, particularly those which include *P. boisei, H. erectus* and, most notably, *H. habilis* (relating to very small sample sizes that may not be representative and yield high standard deviations, see above). Of all samples, *H. naledi* is clearly the most divergent. Although difficult to qualitatively assess, interspecific differences reflect variation across samples in Table 1, including, for example, labial curvature I^1 (range of 0–66.67%), accessory cusps P^3/P^4 (14.79–83.33%), cusp 5 M^1 (0–50%), cusp 7 M_3 (0–56.52%), and root number P_4 (0–100%), among others. Yet, the sample associations in Figure 1 (*A. afarensis*/*A. africanus, P. boisei*/*P. robustus*, earlier and later *Homo* species) also imply some trait uniformity within each of the three genera.

Next, given the apparent efficacy of these findings, we decided to include the Middle Pleistocene *Homo* and Middle/Late Pleistocene *Homo sapiens* samples in a second MMD comparison before trait editing. As above, the intent was to obtain at least some indication of their interspecific affinities. That said, both samples are of patently insufficient size to yield reliable results for this paper, i.e., based on standard recommendations for analysis (above). Instead, these MMD analyses are presented in SOM S1. Based on 62 traits in common across all 11 samples, including a total of 25 with only one observation in the 51 Middle/Late Pleistocene specimens combined, these samples appear most like other fossil *Homo* species;

of these, Middle/Late Pleistocene *Homo sapiens* trends nearest EA and SA *H. sapiens* (SOM Table S1, SOM Figs. S1–S2).

The removal of problematic dental traits was then carried out as previously described. Because of the Plio-Pleistocene focus, all obviously invariant traits were deleted in these particular African fossil samples (i.e., excluding Middle Pleistocene *Homo* and Middle/Late Pleistocene *Homo sapiens*). Examples include: winging I^1, double shoveling I^2, interruption groove I^2, root number M^2, c1–c2 crest M_3, and root number M_3. For brevity, the 16 traits excluded on this basis are listed by their number from Table 1 (i.e., 1, 5, 6, 8, 9, 13, 23, 36, 37, 50, 51, 52, 63, 64, 76, and 78). At the same time, traits with very few observations (see above) were addressed. It is, of course, preferable that only samples of ≥ 10 observations per trait are retained for MMD comparisons (Irish, 2010, 2016). However, such a strategy would reduce the analysis to a single trait comparison (enamel extension UM/LM) across samples. So an alternate approach was taken where deletions were made when multiple samples have fewer than three observations for a trait, e.g., buccal mesial accessory ridge P^4, or any one sample has just one valid observation, e.g., distal accessory ridge C^1 (Table 1). Though not ideal, given the 1) limitations inherent with fossil samples, and 2) capability of the MMD to perform well despite unmet assumptions, this strategy permits at least some assessment of intraspecific variation in the remaining traits. Of these, nine (1, 5, 14, 18, 19, 34, 36, 38, and 64) do not meet these minimum criteria, including four previously removed due to minimal or no variation across samples. As a result, 57 of 78 traits were retained for further editing; the submission of these percentages to PCA identifies additional, though less obvious, non-contributory data.

Seven components with eigenvalues of >1.0 account for 99.12% of the total variance among the nine largest samples. However, the PCA scree plot (not shown) indicates that the first three (68.05% of variance) are most important. The loadings for these traits are listed in

Table 3, where those having strongly positive or negative values of $\geq |0.5|$ drive most of the variation shown in a 3D plot of group component or factor scores (Fig. 2). For component 1, 37 loadings between 0.501 and 0.963 push samples with high percentages of these traits nearer the positive end of the axis labeled as Factor Score 1, namely, *A. afarensis*, *A. africanus*, *P. robustus*, *P. boisei*, and, to a lesser extent, *H. habilis* and *H. erectus*. They are predominantly mass-additive traits associated with morphological complexity of teeth in these species, including labial curvature I^1 (0.594), tuberculum dentale I^1, C^1 (0.690, 0.501), P^3/P^4 accessory cusps (0.756), and so forth (Table 1). On the other hand, much lower occurrences of these same traits, but with a strong loading (-0.500) for grade 4–5 metacone M^3, is characteristic of samples toward the opposite end of this axis: EA and SA *H. sapiens* and *H. naledi*. On Factor Score 2, nine traits possessing highly positive (i.e., 0.503 to 0.943) and 10 with highly negative component 2 loadings (-0.501 to -0.791) show *H. naledi* as unique from other samples. Specifically, the species is characterized by a number of well-expressed principal cusp traits farther back in the molar field, like large M^2 metacone and M^3 hypocone, but few accessory features like tuberculum dentale C^1, cusp 5 M^1, anterior fovea M_1, cusp 7 M_1, and transverse crest P_3. Lastly, strongly positive loadings (0.504–0.803) for the tuberculum dentale I^2, cusp 5 M^1, Carabelli's M^2, protostylid M_3, anterior fovea P_3, and transverse crest P_4, and strongly negative loadings (i.e., -0.501 to -0.653) for shoveling I^1, upper premolar accessory cusps, root number P^3, and cusp number M_1 primarily separate the genera *Australopithecus* and *Paranthropus* on Factor Score 3. Based on these findings, seven of 57 traits submitted to PCA provide little contributory information to assess interspecific variation, so were dropped: shoveling I^2, Carabelli's cusp M^1, parastyle M^1, groove pattern M_3, cusp 7 M_2, upper and lower premolar odontome, and anterior fovea P_4.

In the final step of trait editing, use of Kendall's tau-*b* among the remaining 50 traits revealed high correlations (i.e., $\geq |0.5|$) for: 1) crown asymmetry P_3 with 12 traits ($\tau_b = 0.500$

to 0.784), 2) metaconid placement P_3 with six traits ($\tau_b = 0.502$–0.656), 3) the buccal mesial

accessory ridge P^3 with three traits ($\tau_b = 0.508$–0.609), 4) root number P_3 with three traits ($\tau_b = 0.585$–0.754) including, not unexpectedly, Tomes' root P_3, and 5) protostylid M_2 with

protostylid M_1 ($\tau_b = 0.672$). As a result, these five traits were deleted as well, leaving 45 for

the final MMD comparison as identified in Table 3.

The resulting 45-trait MMD matrix is presented in Table 4. Interspecific variation is

once more evident, with *H. naledi* being the most divergent of all Plio-Pleistocene species.

The small sample of *P. boisei*, after removal of traits with the most missing data and other

editing, now yields pairwise affinities that are more in line with those of *P. robustus,* e.g.,

compare MMD distances with both *Australopithecus* species. However, because of sample

size issues (above), *H. habilis* still exhibits some doubtful pairwise phenetic distances, e.g.,

with *P. boisei* and *P. robustus* (MMD = 0.013 and 0.000; $p \geq 0.025$), although it does remain

phenetically akin to *H. erectus* and *A. afarensis* (MMD = 0.000, $p \geq 0.025$). The latter two

remain close (MMD = 0.053, $p \geq 0.025$), while EA and SA *H. sapiens* retain their similarity

(MMD = 0.011, $p \geq 0.025$). Concerning the MDS solution, Kruskal's stress formula 1 has

increased to 0.095 and r^2 decreased to 0.946, which still indicate an excellent representation

of the matrix (Borgatti, 1997). The interspecific variation illustrated by the new configuration

(Fig. 3) is highly concordant with the 78-trait MDS (Fig. 1), as well as the PCA plot (Fig. 2),

revealing only minor, mostly within-genus sample movement. The consistent relationships of

A. afarensis/*A. africanus*, *P. boisei*/*P. robustus*, and the early and later *Homo* species, again

reflect relative uniformity in trait percentages within each of the three genera (see Table 1).

Discussion and conclusions

Beginning with the quantitative comparisons between *H. naledi* and the eight other

largest samples, the effectiveness of the dental traits and MMD (despite many small sample

sizes of $n < 10$) is evidenced by the similarity of groupings (Figs. 1–3) to those for the same species in earlier studies using cladistic analyses and alternate data (Strait et al., 1997; Strait and Grine, 2004; Smith and Grine, 2008; Berger et al., 2010). Meanwhile, the consistency in patterning from MMD vs. PCA using different numbers of traits further suggests the results are 'real' and not a byproduct of method or illustrative device. Of all comparative samples, *H. naledi* appears most like others within the genus *Homo,* yet is distinct from them given, most noticeably, its extreme position on the Dimension 2 and Factor Score 2 axes. An inspection of individual MMD distances (Tables 2 and 4), focusing on the 45-trait matrix, finds that not only are all pairwise differences significant, but *H. naledi* is most divergent of all non-*Homo sapiens* samples. In the 45-trait matrix the average pairwise distance between *H. naledi* and the six other Plio-Pleistocene samples is 0.445; the same value among the latter six is just 0.111. In the taxonomic description of *H. naledi* from the Dinaledi Chamber, Berger et al. (2015:20, 24) provided a summary of features likely responsible for this divergence, i.e., the teeth "are not only small, but markedly simple in crown morphology," with a lack of "many derived features shared by [Middle] and [Late Pleistocene] *Homo* and *H. sapiens*" (below). This same patterning is evident in crowns of specimens from the Lesedi Chamber (Hawks et al., 2017).

Sample sizes must be considered, but this description is quantified in Table 1, where 36 of 78 traits are absent in *H. naledi*, most of which are present in other fossil and/or recent samples—in many cases at high frequencies: labial curvature I^1, tuberculum dentale C^1, cusp 5 M^1, Carabelli's cusp M^3, multiple P_4 lingual cusps, anterior fovea M_1, 6-cusped M_1, 7-cusped M_3, deflecting wrinkle M_1 and M_3, cusp 7 M_1–M_3, 2-rooted P_4, metaconid placement P_3, transverse crest P_3–P_4, and asymmetry P_3–P_4. Most of these can be considered accessory or mass-additive traits (above). Additional traits that are present but at much lower rates than in other samples, notably the older species on the left of Table 1, include: accessory cusps

P^3/P^4, cusp 5 M^2, 6-cusped M_2, deflecting wrinkle M_2, protostylid M_2–M_3, grade 1 enamel extension on upper and lower molars, and buccal median ridge P^4. This is not to say that no 'accessory' traits occur frequently in *H. naledi*, e.g., C^1 double shoveling, C^1 distal accessory ridge, and perhaps upper premolar buccal accessory ridges. That said, as noted in the PCA results and indicated by loadings in Table 3, especially Component 2, the species exhibits the highest or one of the highest percentages of traits relating to retention and expression of the principal (or main) cusps, as well as roots. Though not a cladistic study, such traits are known to be plesiomorphic (see full reference list in Irish, 1997; Irish and Guatelli-Steinberg, 2003) based on their presence in various fossil hominins and extinct and extant non-human primates (as are many of those listed above). They include: little or no reduction of root number in P^3–M^3, P_3, and M_1–M_3, along with a lack of reduction of the M^1–M^3 metacones and hypocones (grades 4-5) and presence of the fifth principal cusp, plus Y-pattern on M_1–M_3 (Fig. 4).

Qualitative comparisons between *H. naledi* and the two pencontemporaneous samples (Table 1), Middle Pleistocene *Homo* and Middle/Late Pleistocene *Homo sapiens*, support the above findings—at least based on those teeth with multiple observations. *Homo naledi* shares a number of similar percentages with one or both samples, including: little or no occurrence of cusp 5 M^1, Carabelli's cusp M^3, 7-cusped M_3, deflecting wrinkle M_3, enamel extensions, torsomolar angle M_3, and asymmetry P_4, along with prevalent protostylid M_3, (perhaps) root number P_4–M_3, metaconid placement P_4, and metaconid height P_3–P_4. On the other hand, *H. naledi* also shows some obvious distinction from these *Homo* samples by the: 1) frequent presence of principal cusps, such as metacone M^2–M^3, hypocone M^2–M^3, and hypoconulid with Y-pattern on M_1–M_3, and 2) overall lack of accessory cusps and crown features like cusp 5 M^2, multiple P_4 lingual cusps, anterior fovea M_1, 6-cusped M_1, deflecting wrinkle M_1, cusp 7 M_1–M_3, metaconid placement P_3, and transverse crest P_3–P_4. Again, refer to SOM S1, Table S1 and Figures S1–S2. As mentioned, these two comparative samples are limited by

the overall lack of such African specimens, particularly Middle Pleistocene *Homo*. Other data exist; for example, Martinón-Torres et al. (2012) used the ASUDAS to record traits in the Middle Pleistocene Sima de los Huesos (SH) hominins, a very small sample of other European *Homo heidelbergensis* (HEI), and European Neanderthals (NEA), among others. However, because of, for example, the "highly derived and Neanderthal character of the Sima de los Huesos dentitions" (Martinón-Torres et al., 2012:55), it was assumed that these samples are too disparate to supplement the African data; this was found to be a valid concern based on marked differences in percentages for many of the 50 traits in common between studies (see SOM S2 and Table S2). Further, an MMD comparison of the data yields large, significantly different distances between SH, HEI, and NEA and the five largest *Homo* samples from the present study (SOM Table S3 and Fig. S3), including *H. naledi*. Another MMD comparison including Middle Pleistocene *Homo* and Middle/Late Pleistocene *Homo sapiens*, based on 41 traits in common, provides additional support; some similarity to the HEI sample is suggested (SOM S3, Table S4, and Fig. S4), but sample size issues are likely contributory.

Overall, the present phenetic findings parallel those of Thackeray (2015)—based on cranial data—and Dembo et al. (2016)—based on the phylogenetic analyses of craniodental characters. When dental samples are compared simultaneously, for example in Figure 3, *H. naledi* most closely groups with other members of the genus *Homo*. Nevertheless, the species possesses combinations and expressions of traits that serve to distinguish it from the latter, as indicated by the intersample distances (Table 4). As Berger et al. (2015) and Hawks et al. (2017) described (also see Schroeder et al., 2017), beyond dental traits the *H. naledi* crania and postcrania present a mixture of shared and unique features relative to other *Homo* species, including: a well-developed and arched supraorbital torus that is separated from the vault by a continuous supratoral sulcus like in *H. habilis* and *H. erectus*, marked angular and

occipital tori like *H. erectus*, and some facial similarities to *H. rudolfensis.* That said, the cranium does not have many characteristics of more recent *Homo* including, notably, large cranial capacity (Garvin et al., 2017). In the postcranial skeleton, *Homo*-like features include relatively long lower limbs, muscle attachments indicative of a striding gate, and modern aspects of the ankles, feet, and hands; other traits are reminiscent of earlier species, including curved phalanges, wide lower thorax, and ape-like upper limbs (Berger et al., 2015; Harcourt-Smith et al., 2015; Kivell et al, 2015; Feuerriegel et al., 2017; Garvin et al., 2017; Williams et al., 2017; Hawks et al., 2017).

Dental affinities among the eight largest comparative samples are also of interest. As stated, interspecific patterning is consistent with that in earlier studies (Figs. 1–3). However, the MMD distances, beyond indicating the individuality of *H. naledi,* are telling. The 45-trait matrix is again emphasized (Table 4) and, certainly for this specific portion of the discussion, the make-up of the pooled *H. erectus* sample should be considered (above). The Holocene samples of EA and SA *H. sapiens* do not differ significantly from each other (MMD = 0.011, $p \geq 0.025$), as may be expected with contemporary members of the same species in relatively proximate geographic regions. They differ significantly from all Plio-Pleistocene samples, but are most similar to others within the genus *Homo*, where the MMD distances from lowest to highest are: *H. erectus* (with SA *H. sapiens* = 0.346; EA *H. sapiens* = 0.428), *H. habilis* (SA *H. sapiens* = 0.371; EA *H. sapiens* = 0.438), and finally *H. naledi* (SA *H. sapiens* = 0.586; EA *H. sapiens* = 0.591). Both SA and EA *H. sapiens* are highly distinct from the older and/or dead-end species *A. afarensis*, *A. africanus*, *P. boisei*, and *P. robustus* (range 0.689–0.967, mean MMD = 0.867). Also suggestive of a temporal component in these affinities, *H. erectus* and *H. habilis* are closer to the latter four, older samples (MMD = 0.000–0.230), although with one exception *H. erectus,* at least, differs significantly from them.

Beyond comparative purposes with *H. naledi,* it would clearly be important to obtain larger, more representative African and other Middle Pleistocene samples (though again see SOM S2–S3) to more fully discern diachronic relatedness. Small sample size is also a factor in the better-represented samples, most conspicuously *H. habilis* and its implausible, insignificant distances with *P. boisei, P. robustus*, and perhaps *Australopithecus* (e.g., MMD = 0.000-0.108, $p \geq 0.025$); analogous size-influenced affinities between samples that were otherwise documented to be divergent have been reported in previous studies (Irish, 1993, 2005, 2006, 2010; Irish et al., 2014b). That is, small sample sizes can reduce individual MMD distances, but most often increase the standard deviation that, given the significance formula (above), can yield a type II error; therefore, the MDS and PCA patterning among samples (Figs. 1–3) figures to be a better, overall indicator of interspecific variation. Nevertheless, the *A. afarensis* sample, as compiled here, appears to be more similar to *H. habilis,* as well as *H. erectus,* than was revealed in the abovementioned cladistic study (Irish et al., 2013); fewer ($n = 18$) traits in the latter study and standard coding, which does not address intraspecific variability to the level in the present analyses, likely played a role. The remaining affinities are not unexpected, based on the proximity of the *Australopithecus* and *Paranthropus* samples in all figures.

To conclude, the original qualitative taxonomic description (Berger et al., 2015), later quantitative analyses (Thackeray, 2015; Dembo, 2016), description of additional specimens (Hawks et al., 2017), and current dental nonmetric study of African samples (including SOM S1–S3) all provide generally concordant findings to support the inclusion of *H. naledi* in the genus *Homo*; or, said another way, there is little to suggest it does not belong in the genus. The relatively recent dates (Dirks et al., 2017) of the Dinaledi remains may also be indirectly supportive of this taxonomic classification, unless a relict *Australopithecus* population survived into the Middle Pleistocene or future phylogenetic research finds the hominins

unique enough to warrant naming a separate genus. The designation of *H. naledi* as a taxonomically valid species of *Homo* is also supported by the combination of cranial, dental, and postcranial characteristics (above) relative to other members of the genus. The likelihood of population homogeneity must be considered, but the highly uniform pattern of crown and root morphology in all specimens of *H. naledi* is, on its own, indicative of the species' distinctiveness. None of the other samples in this study (also see SOM S2) exhibit an equivalent combination of small teeth with retention and full expression of the principal cusps on all molars, yet the absence of accessory and other traits known to be plesiomorphic in both African fossil and recent hominins; indeed, the samples of Holocene *H. sapiens* in the present study (Irish et al., 2014), which have smaller teeth than *H. naledi* (compare mean crown diameters in Irish et al., 2016:Table 2 with those in Berger et al., 2015:Table 2), evidence such accessory, plesiomorphic features (e.g., labial curvature UI1, cusp-7 LM, etc.; Irish, 1993, 1997, 1998, 2013). Therefore, again, *H. naledi* appears dentally distinct relative to these other species. Lastly, interspecific groupings of the other samples are comparable to those in previously published studies. Future comparative analyses will benefit from the collection of additional data not currently presented here—particularly Middle Pleistocene contemporaries of *H. naledi*. Different quantitative and illustrative methods, as stated in the Introduction, can then be used with these data to further discern relatedness; the goal, simply, is to better understand where and how *H. naledi* fits in.

Acknowledgements

References

Abdi, H., Williams, L.J., 2010. Principal Component Analysis. WIREs Computational Statistics 2, 433–459.

Asfaw, B., White, T., Lovejoy, O., Latimer, B., Simpson, S., Suwa, G., 1999. *Australopithecus garhi*: a new species of early hominid from Ethiopia. Science 284, 629–635.

Baab, K.L., 2008. The taxonomic implications of cranial shape variation in *Homo erectus*. Journal of Human Evolution 54, 827–847.

Bailey, S.E., 2000. Dental morphological affinities among late Pleistocene and recent humans. Dental Anthropology 14, 1–8.

Bailey, S.E., 2002a. A closer look at Neanderthal postcanine dental morphology: the mandibular dentition. Anatomical Record 269, 148–156.

Bailey, S.E., 2002b. Neandertal dental morphology: implications for modern human origins. Ph.D. Dissertation, Arizona State University.

Bailey, S.E., Hublin, J.J., 2013. 10 What does it mean to be dentally "modern"? In: Scott, G.R., Irish J.D., (Eds.), Anthropological Perspectives on Tooth Morphology: Genetics, Evolution, Variation. Cambridge University Press, Cambridge, pp. 222–249.

Bailey, S.E., Lynch, J.M., 2005. Diagnostic differences in mandibular P4 shape between Neandertals and anatomically modern humans. American Journal of Physical Anthropology 126, 268–277.

Berger, L.R., Parkington, J.E. 1995. Brief communication: a new Pleistocene hominid-bearing locality at Hoedjiespunt, South Africa. American Journal of Physical Anthropology 98, 601–609.

Berger, L.R., de Ruiter, D.J., Churchill, S.E., Schmid, P., Carlson, K.J., Dirks, P.H., Kibii, J.M., 2010. *Australopithecus sediba*: a new species of *Homo*-like australopith from South Africa. Science 328, 195–204.

Berger, L.R., Hawks, J., de Ruiter, D.J., Churchill, S.E., Schmid, P., Delezene, L.K., Kivell, T.L., Garvin, H.M., Williams, S.A., DeSilva, J.M., Skinner, M.M., Musiba, C.M., Cameron, N., Holliday, T.W., Harcourt-Smith, W., Ackermann, R.R., Bastir, M., Bogin, B., Bolter, D., Brophy, J., Cofran, Z.D., Congdon, K.A., Deane, A.S., Dembo, M., Drapeau, M., Elliott, M.C., Feuerriegel, E.M., Garcia-Martinez, D., Green, D.J., Gurtov, A., Irish, J.D., Kruger, A., Laird, M.F., Marchi, D., Meyer, M.R., Nalla, S., Negash, E.W., Orr, C.M., Radovcic, D., Schroeder, L., Scott, J.E., Throckmorton, Z., Tocheri, M.W., VanSickle, C., Walker, C.S., Wei, P., Zipfel, B., 2015. *Homo naledi*, a new species of the genus *Homo* from the Dinaledi Chamber, South Africa. eLife 4, e09560.

Bermúdez de Castro, J.M., 1989. The Carabelli trait in human prehistoric populations of the Canary Islands. Human Biology 61, 117–131.

Bermúdez de Castro, J.M., Martinón-Torres, M., Gómez-Robles, A., Prado, L. Sarmiento, S., 2007. Comparative analysis of the Gran Dolina-TD6 (Spain) and Tighennif (Algeria) hominin mandibles. Bulletins et Mémoires de la Société d'Anthropologie de Paris 19, 149167.

Borg, I., Groenen, P., 1997. Modern Multidimensional Scaling. Springer-Verlag, New York.

Borgatti, S.P. 1997. Multidimensional Scaling. www.analytictech.com/borgatti/mds.htm

Braga, J., Thackeray, J.F. 2003. Early *Homo* at Kromdraai B: probabilistic and morphological analysis of the lower dentition. Comptes Rendus Palevol 2, 269–279.

Bräuer, G., Mehlman, M.J., 1988. Hominin molars from a Middle Stone Age level at the

    Mumba Rock Shelter, Tanzania. American Journal of Physical Anthropology 75, 69–76.

Burnett, S.E., Irish, J.D., Fong, M.R., 2013. Wears the problem? Examining the effect of

    dental wear on studies of crown morphology. In: Scott, G.R., Irish J.D., (Eds.),

    Anthropological Perspectives on Tooth Morphology: Genetics, Evolution, Variation.

    Cambridge University Press, Cambridge, pp. 535–553.

Burnett, S.E., 2016. Crown wear: Identification and categorization. In: Irish J.D., Scott GR,

    (Eds.), A Companion to Dental Anthropology. Wiley Blackwell, London, pp. 415–432.

Carter, K., Worthington, S., Smith, T.M., 2014. News and views: Non-metric dental traits and

    hominin phylogeny. Journal of Human Evolution 69, 123–128.

Cohen, J., 1988. Statistical Power Analysis for the Behavioral Sciences. 2nd ed. Erlbaum,

    Hillsdale.

Cox, T.F., Cox, M.A.A., 1994. Multidimensional Scaling. Chapman and Hall, London.

Curnoe, D., 2010. A review of early *Homo* in southern Africa focusing on cranial,

    mandibular and dental remains, with the description of a new species (*Homo gautengensis*

    sp. nov.). Homo J. Comp. Human Biology 61, 151–177.

Dembo, M., Radovčić, D., Garvin, H.M., Laird, M.F., Schroeder, L., Scott, J.E., Brophy, J.,

    Ackermann, R.R., Musiba, C.M., de Ruiter, D.J., 2016. The evolutionary relationships and

    age of *Homo naledi*: An assessment using dated Bayesian phylogenetic methods. Journal

    of Human Evolution 97, 17–26.

Dirks, P., Roberts, E.M., Hilbert-Wolf, H., Kramers, J.D., Hawks, J., Dosseto, A., Duval, M.,

    Elliott, E.M., Grün, R., Hellstrom, J., Herries, A.I.R., Joannes-Boyau, R., Placzek, C.J.,

Robbins, J., Spandler, C., Wiersma, J., Woodhead, J., Berger, L.R., 2017. The age of *Homo naledi* and associated sediments in the Rising Star Cave, South Africa. eLife 6, e24231.

Feuerriegel, E.M., Green, D.J., Walker, C.S., Schmid, P., Hawks, J., Berger, L.R., Churchill, S.E., 2017. The upper limb of *Homo naledi*. Journal of Human Evolution 104, 155–173.

Garvin, H., Elliott, M., Delezene, L.K., Hawks, J., Churchill, S., Berger, L., Holliday, T., 2017. Body size, brain size, and sexual dimorphism in *Homo naledi*. Journal of Human Evolution 111, 119–138.

Geraads, D., Hublin, J.J., Jaeger, J.J., 1986. The Pleistocene hominid site of Ternifine Algeria: new results on the environment, age, and human industries. Quaternary Research 25, 380–386.

Gordon, A.D., Wood, B.A. 2013. Evaluating the use of pairwise dissimilarity metrics in paleoanthropology. Journal of Human Evolution 65, 465–477.

Green, R., Suchey, J., 1976. The use of inverse sine transformation in the analysis of non-metrical data. American Journal of Physical Anthropology 45, 61–68.

Green, R., Suchey, J., Gokhale. D., 1979. The statistical treatment of correlated bilateral traits in the analysis of cranial material. American Journal of Physical Anthropology 50, 629–634.

Grine, F.E., 2000. Middle Stone Age human fossils from Die Kelders Cave 1, Western Cape Province, South Africa. Journal of Human Evolution 38, 129–145.

Grine, F.E., 2012. Observations on Middle Stone Age human teeth from Klasies River Main Site, South Africa. Journal of Human Evolution 63, 750–758.

Grine, F.E., Klein, R.G., 1985. Pleistocene and Holocene human remains from Equus Cave, South Africa. Anthropologie 8, 55–98.

Grine, F.E., Klein, R.G., 1993. Late Pleistocene human remains from the Sea Harvest site, Saldanha Bay, South Africa. South African Journal of Science 89, 145–152.

Guatelli-Steinberg, D., Hunter, J.P., Durner, R.M., Moormann, S., Weston, T., Betsinger, T.K., 2013. Teeth, morphogenesis, and levels of variation in the human Carabelli's trait. In: Scott, G.R., Irish, J.D., (Eds.), Anthropological Perspectives on Tooth Morphology: Genetics, Evolution, Variation. Cambridge University Press, Cambridge, pp. 69–91.

Haeussler, A.M., Turner, C.G. II, Irish, J.D., 1988. Concordance of American and Soviet methods in dental anthropology. American Journal of Physical Anthropology 75, 218.

Hanihara, T., 1992. Dental and cranial affinities among populations of East Asia and the Pacific: The basic populations in East Asia, IV. American Journal of Physical Anthropology 88, 163–182.

Harcourt-Smith, W., Throckmorton, Z., Congdon, K., Zipfel, B., Deane, A.S., Drapeau, M., Churchill, S., Berger, L., DeSilva, J., 2015. The foot of *Homo naledi*. Nature Communications 6, 8432.

Harris, E.F., Sjøvold, T., 2004. Calculation of Smith's mean measure of divergence for intergroup comparisons using nonmetric data. Dental Anthropology 17, 83–93.

Hawks, J., Elliott, M., Schmid, P., Churchill, S.E., de Ruiter, D.J., Roberts, E.M., Hilbert-Wolf, H., Garvin, H.M., Williams, S.A., Delezene, L.K., Feuerriegel, E.M., Randolph-Quinney, P., Kivell, T.L., Laird, M.F., Tawane, G., DeSilva, J.M., Bailey, S.E., Brophy, J.K., Meyer, M.R., Skinner, M.M., Tocheri, M.W., VanSickle, C., Walker, C.S.,

Campbell, T.L., Kuhn, B., Kruger, A., Tucker, S. Gurtov, A., Hlophe, N., Hunter, R., Morris, H., Peixotto, B., Ramalepa, M., van Rooyen, D., Tsikoane, M., Boshoff, P., Dirks, P.H.G.M., Berger, L.R., 2017. New fossil remains of *Homo naledi* from the Lesedi Chamber, South Africa. eLife 6, e24232.

Hintze, J.L., 2007. NCSS Help System. NCSS, Kaysville, Utah.

Hubbard, A.R., Guatelli-Steinberg, D., Irish, J.D., 2015. Do nuclear DNA and dental nonmetric data produce similar reconstructions of regional population history? An example from modern coastal Kenya. American Journal of Physical Anthropology 157, 295–304.

Hublin, J.J., Ben-Ncer, A., Bailey, S.E., Freidline, S.E., Neubauer, S., Skinner, M.M., Bergmann, I., Le Cabec, A., Benazzi, S., Harvati, K. Gunz, P., 2017. New fossils from Jebel Irhoud, Morocco and the pan-African origin of *Homo sapiens*. Nature 546, 289–292.

Hughes, T.E., Townsend, G.C., 2013a. Twin studies of dental crown morphology: Genetic and environmental determinants of the Cusp of Carabelli. Bulletin of the International Association of Paleodontology 7, 87.

Hughes, T.E., Townsend, G.C., 2013b. Twin and family studies of human dental crown morphology: genetic, epigenetic, and environmental determinants of the modern human dentition. In: Scott, G.R., Irish J.D., (Eds.), Anthropological Perspectives on Tooth Morphology: Genetics, Evolution, Variation. Cambridge University Press, Cambridge, pp. 31–68.

IBM Corp. Released 2016. IBM SPSS Statistics for Windows, Version 24.0. Armonk, NY: IBM Corp.

Irish J.D., 1993. Biological affinities of late Pleistocene through modern African aboriginal

populations: The dental evidence. Ph.D. Dissertation, Arizona State University.

Irish, J.D., 1997. Characteristic high- and low-frequency dental traits in sub-Saharan African

populations. American Journal of Physical Anthropology 102, 455–467.

Irish, J.D., 1998. Ancestral dental traits in recent Sub-Saharan Africans and the origins of

modern humans. Journal of Human Evolution 34, 81–98.

Irish, J.D., 2005. Population continuity versus discontinuity revisited: Dental affinities among

Late Paleolithic through Christian era Nubians. American Journal of Physical

Anthropology 128, 520-–35.

Irish, J.D., 2006. Who were the ancient Egyptians? Dental affinities among Neolithic through

post- dynastic peoples. American Journal of Physical Anthropology129, 529–543.

Irish, J.D., 2010. The mean measure of divergence: Its utility in model-free and model-bound

analyses relative to the Mahalanobis D^2 distance for nonmetric traits. American Journal of

Human Biology 22, 378–395.

Irish, J.D., 2013. Afridonty: the "Sub-Saharan African Dental Complex" revisited. In: Scott,

G.R., Irish J.D., (Eds.), Anthropological Perspectives on Tooth Morphology: Genetics,

Evolution, Variation. Cambridge University Press, Cambridge, pp. 278–295.

Irish, J.D., 2016. Who were they really? Model-free and model-bound dental nonmetric

analyses to affirm documented population affiliations of seven South African "Bantu"

samples. American Journal of Physical Anthropology 159, 655–670.

Irish, J.D., Black, W., Sealy, J., Ackermann, R., 2014b. Questions of Khoesan continuity: Dental affinities among the indigenous Holocene peoples of South Africa. American Journal of Physical Anthropology 155, 33–44.

Irish, J.D., Guatelli-Steinberg, D., 2003. Ancient teeth and modern human origins: an expanded comparison of African Plio-Pleistocene and recent world dental samples. Journal of Human Evolution 45, 113–144.

Irish, J.D., Guatelli-Steinberg, D., Legge, S.S., de Ruiter, D.J., Berger, L.R., 2013. Dental morphology and the phylogenetic "place" of *Australopithecus sediba*. Science 340, 1233062.

Irish, J.D., Guatelli-Steinberg, D., Legge, S.S., de Ruiter, D.J., Berger, L.R., 2014a. Response to 'Non-metric dental traits and hominin phylogeny' by Carter et al., with additional information on the Arizona State University Dental Anthropology System and phylogenetic 'place' of *Australopithecus sediba*. Journal of Human Evolution 69, 9–134.

Irish, J.D., Hemphill, B.E., de Ruiter, D.J., Berger, L.R., 2016. The apportionment of tooth size and its implications in *Australopithecus sediba* versus other Plio-Pleistocene and recent African hominins. American Journal of Physical Anthropology 161, 398–413.

Johanson, D.C., White, T.D., Coppens, Y., 1982. Dental remains from the Hadar Formation, Ethiopia: 1974–1977 collections. American Journal of Physical Anthropology 57, 545–603.

Kimbel, W.H., Delezene, L.K., 2009. "Lucy" redux: A review of research on *Australopithecus afarensis*. American Journal of Physical Anthropology 140, 2–48.

Kivell, T.L., Deane, A.S., Tocheri, M.W., Orr, C.M., Schmid, P., Hawks, J., Berger, L.R., Churchill, S.E., 2015. The hand of *Homo naledi*. Nature Communication 6, 8431.

Konigsberg, L.W., 1990. Analysis of prehistoric biological variation under a model of isolation by geographic and temporal distance. Human Biology 62, 49–70.

Kruskal, J.B., Wish, M., 1978. Multidimensional Scaling. Sage Publications, Beverly Hills.

Larsen, C.S., 1997. Bioarchaeology. Cambridge University Press, Cambridge.

Leakey, L.S.B., 1935. The Stone Age Races of Kenya. Oxford University Press, London.

Leigh, S.R., Relethford, J.H., Park, P.B., Konigsberg, L.W. 2003. Morphological differentiation of *Gorilla* subspecies. In: Taylor, A.B., Goldsmith, M.L. (Eds.), Gorilla Biology: A Multidisciplinary Perspective. Cambridge University Press, Cambridge, pp. 104–131.

Little, R.J., Rubin, D.B., 2014. Statistical Analysis with Missing Data. John Wiley & Sons, New York.

Livingstone, F.B., 1991. Phylogenies and the forces of evolution. American Journal of Human Biology 3, 83–89.

Lockwood, C.A., Tobias, P.V., 2002. Morphology and affinities of new hominin cranial remains from Member 4 of the Sterkfontein Formation, Gauteng Province, South Africa. Journal of Human Evolution 42, 389–450.

Martinón-Torres, M., Bermúdez de Castro, J., Gómez-Robles, A., Arsuaga, J., Carbonell, E., Lordkipanidze, D., Manzi, G., Margvelashvili, A., 2007. Dental evidence on the hominin

38

dispersals during the Pleistocene. Proceedings of the National Academy of Science 104, 13279–13282.

Martinón-Torres, M., Bermúdez de Castro, J., Gómez-Robles, A., Margvelashvili, A., Prado, L., Lordkipanidze, D., Vekua, A., 2008. Dental remains from Dmanisi (Republic of Georgia): morphological analysis and comparative study. Journal of Human Evolution 55, 249–273.

Martinón-Torres, M., Bermúdez de Castro, J.M., Gómez-Robles, A., Prado-Simón, L., Arsuaga, J.L., 2012. Morphological description and comparison of the dental remains from Atapuerca-Sima de los Huesos site (Spain). Journal of Human Evolution 62, 7–58.

Martinón-Torres, M., Bermúdez de Castro, J.M., Martín-Francés, L., Gracia-Téllez, A., Martinez, I., Arsuaga, J.L., 2013. Dental morphology of European Middle Pleistocene populations. In: Scott, G.R., Irish J.D. (Eds.), Anthropological Perspectives on Tooth Morphology: Genetics, Evolution, Variation. Cambridge University Press, Cambridge, pp. 201–221.

McBurney, C.B., Trevor, J.C., Wells, L.H., 1953. The Haua Fteah fossil jaw. Journal of the Royal Anthropological Institute of Great Britain and Ireland 83, 71-85.

Moggi-Cecchi, J., Grine, F.E., Tobias, P.V., 2006. Early hominid dental remains from Members 4 and 5 of the Sterkfontein Formation (1966–1996 excavations): catalogue, individual associations, morphological descriptions and initial metrical analysis. Journal of Human Evolution 50, 239–328.

Moggi-Cecchi, J., Menter, C., Boccone, S., Keyser, A., 2010. Early hominin dental remains from the Plio-Pleistocene site of Drimolen, South Africa. Journal of Human Evolution 58, 374–405.

Morris, A.G., 2002. Isolation and the origin of the Khoisan: Late Pleistocene and Early Holocene human evolution at the southern end of Africa. Human Evolution 17, 231–240.

Morris, A.G., 2003. The myth of the East African 'Bushmen'. South African Archaeological Bulletin 58, 85–90.

Nichol, C.R., 1990. Dental genetics and biological relationships of the Pima Indians of Arizona. Ph.D. Dissertation, Arizona State University.

Nichol, C.R., Turner, II, C.G., 1986. Intra- and interobserver concordance in classifying dental morphology. American Journal of Physical Anthropology 69, 299–315.

Oujaa, A., Arnaud, J., Bardey-Vaillant, M., Grimaud-Hervé, D. 2017. The fossil human from Rabat-Kébitat (Morocco): Comparative study of the cranial and mandibular fragments. African Archaeological Review 34, 511–523.

Randolph-Quinney, P.S., 2015a. The mournful ape: Conflating expression and meaning in the mortuary behaviour of *Homo naledi*. South African Journal of Science 111, #a0131.

Randolph-Quinney, P.S., 2015b. A new star rising: Biology and mortuary behaviour of *Homo naledi*. South African Journal of Science 111, #a0122.

Rathmann, H., Reyes-Centeno, H., Ghirotto, S., Creanza, N., Hanihara, T., Harvati, K. 2017. Reconstructing human population history from dental phenotypes. Science Reports 7, 12495.

Raynal, J.P., Sbihi-Alaoui, F.Z., Mohib, A., El Graoui, M., Lefèvre, D., Texier, J.P., Geraads, D., Hublin, J.J., Smith, T., Tafforeau, P. and Zouak, M., 2010. Hominid Cave at Thomas Quarry I (Casablanca, Morocco): recent findings and their context. Quaternary International 223, 369–382.

Reid, G., Sidwell, K., 2002. Overlapping variables in botanical systematics. In: Macleod, N., Forey, P.L. (Eds,) Morphology, Shape and Phylogeny. Taylor & Francis, London, pp. 53–66.

Relethford, J.R., 1994. Craniometric variation among modern human populations. American Journal of Physical Anthropology 95, 53–62.

Relethford, J.R., 2001. Global analysis of regional differences in craniometric diversity and population substructure. Human Biology 73, 626–636.

Richter, D., Grün, R., Joannes-Boyau, R., Steele, T.E., Amani, F., Rué, M., Fernandes, P., Raynal, J-P., Geraads, D., Ben-Ncer, A., Hublin, J-J., McPherron, S.P., 2017. The age of the hominin fossils from Jebel Irhoud, Morocco, and the origins of the Middle Stone Age. Nature 546, 293–296.

Rightmire, G.P., 1991. Comparative studies of Late Pleistocene human remains from Klasies River Mouth, South Africa. Journal of Human Evolution 20, 131–156.

Rightmire, G.P., 1999. Dental variation and human history. Revista Archaeologica 20, 1–3.

Rightmire, G.P., Lordkipanidze, D., 2010. The first hominin colonization of Eurasia. In: Fleagle, J.G., Shea, J.J., Grine, F.E., Baden, A.L., Leakey, R.E., (Eds.), Out of Africa I: The First Hominin Colonization of Eurasia. Springer, New York, pp. 225–243.

Rightmire, G.P., Lordkipanidze, D., Vekua, A., 2006. Anatomical descriptions, comparative studies and evolutionary significance of the hominin skulls from Dmanisi, Republic of Georgia. Journal of Human Evolution 50, 115–141.

Robbins, L.H., Angel, J. L., Phenice, T. W., and Lynch, B.M., 1980. Lopoy and Lothagam. Michigan State University, Lansing.

Romesburg, C.H., 1984. Cluster Analysis for Researchers. Lifetime Learning Publications,
Belmont.

Schols, P., D'hondt, C., Geuten, K., Merckx, V., Janssens, S., Smets, E., 2004. MorphoCode:
coding quantitative data for phylogenetic analysis. PhyloInformatics 4, 1-4.

Schroeder, L., Scott, J.E., Garvin, H.M., Laird, M.F., Dembo, M., Radovčić, D., Berger, L.R.,
de Ruiter, D.J., Ackermann, R.R., 2017. Skull diversity in the *Homo* lineage and the
relative position of *Homo naledi*. Journal of Human Evolution 104, 124–135.

Schwartz, J.H., 2015. Why the *Homo naledi* discovery may not be quite what it seems.
Newsweek, http://europe.newsweek.com/why-homo-naledi-discovery-may-not-be-quite-
what-it-seems-332804 (accessed 10 September 2015).

Scott, G.R., 1973. Dental morphology: A genetic study of American white families and
variation in living Southwest Indians. Ph.D. Dissertation, Arizona State University.

Scott, G.R., 1980. Population variation of Carabelli's trait. Human Biology 52, 63–78.

Scott, G.R., Irish, J.D., 2017. Human Tooth Crown and Root Morphology: The Arizona State
University Dental Anthropology System. Cambridge University Press, Cambridge.

Scott, G.R., Maier, C., Heim, K., 2016. Identifying and recording key morphological
(nonmetric) crown and root traits. In: Irish J.D., Scott GR, (Eds.), A Companion to Dental
Anthropology. Wiley Blackwell, London, pp. 245–264.

Scott, G.R., Turner, C.G., 1997. The Anthropology of Modern Human Teeth: Dental
Morphology and its Variation in Recent Human Populations. Cambridge University Press,
Cambridge.

Scott, G.R, Yap Potter RH, Noss JF, Dahlberg AA, Dahlberg T., 1983. The dental morphology of Pima Indians. American Journal of Physical Anthropology 61, 13–31.

Sjøvold T., 1973. Occurrence of minor non-metrical variants in the skeleton and their quantitative treatment for population comparisons. Homo 24, 204–233.

Sjøvold, T., 1977. Non-metrical divergence between skeletal populations: the theoretical foundation and biological importance of C. A. B. Smith's mean measure of divergence. Ossa 4, 1–133.

Smith, P., Shegev, M., 1988. The dentition of Nubians from Wadi Halfa, Sudan: An evolutionary perspective. Journal of the Dental Association of South Africa 43, 539–541.

Smith, P., Brink, J.S., Hoffman, J.S., Bam, L.C., Nshimirimana, R., de Beer, F.C., 2015. The late Middle Pleistocene upper third molar from Florisbad: metrics and morphology. Transactions of the Royal Society of South Africa 70, 233–244.

Smith, H.F., Grine, F.E., 2008. Cladistic analysis of early *Homo* crania from Swartkrans and Sterkfontein, South Africa. Journal of Human Evolution 54, 684–704.

Smith, T.M., Tafforeau, P., Reid, D.J., Grün, R., Eggins, S., Boutakiout, M., Hublin, J.J., 2007. Earliest evidence of modern human life history in North African early *Homo sapiens*. Proceedings of the National Academy of Science 104, 6128–6133.

Stojanowski CM, Johnson KM., 2015. Observer error, dental wear, and the inference of New World Sundadonty. American Journal of Physical Anthropology 156, 349–362.

Strait, D.S., Grine, F.E., 2004. Inferring hominoid and early hominid phylogeny using craniodental characters: the role of fossil taxa. Journal of Human Evolution 47, 399–452.

Strait, D.S., Grine, F.E., Moniz, M.A., 1997. A reappraisal of early hominid phylogeny. Journal of Human Evolution 32, 17–82.

Stringer, C., Humphrey, L., Compton, T., 1997. Cladistic analysis of dental traits in recent humans using a fossil outgroup. Journal of Human Evolution 32, 389–402.

Stynder, D.D., Ackermann, R.R., Sealy, J.C., 2007. Craniofacial variation and population continuity during the South African Holocene. American Journal of Physical Anthropology 134, 48970500.

Thackeray, F., 2007. Approximation of a biological species constant? South African Journal of Science 103, 489.

Thackeray, F., 2015. Estimating the age and affinities of *Homo naledi*. South African Journal of Science 111, #a0124.

Templeton, A.R., 1999. Human races: a genetic and evolutionary perspective. American Anthropologist 100, 632–650.

Thiele, K., 1993. The holy grail of the perfect character: the cladistic treatment of morphometric data. Cladistics 9, 275–304.

Tobias, P.V., 1971. Human skeletal remains from the Cave of Hearths, Makapansgat, Northern Transvaal. American Journal of Physical Anthropology 34, 335–368.

Tobias, P.V., 1991. The Skulls, Endocasts, and Teeth of *Homo habilis*: pt. 1-4. Cambridge University Press, Cambridge.

Turner, C.G. II, Scott, G.R., 1977. Dentition of Easter Islanders. In: Dahlberg, A.A., Graber, T.M., (Eds.), Orofacial Growth and Development. The Hague, Mouton, pp. 229–249.

Turner, C.G. II., 1985. The dental search for Native American origins. In: Kirk, R., Szathmary, E. (Ed.), Out of Asia. Journal of Pacific History, Canberra, pp. 31–78.

Turner, C.G. II., 1987. Late Pleistocene and Holocene population history of East Asia based on dental variation. American Journal of Physical Anthropology 73, 305–322.

Turner, C.G., Nichol, C.R., Scott, G.R., 1991. Scoring procedures for key morphological traits of the permanent dentition: the Arizona State University dental anthropology system. In: Kelley, M.A., Larsen, C.S. (Eds.), Advances in Dental Anthropology. Wiley-Liss, New York, pp. 13–32.

Val, A., 2016. Deliberate body disposal by hominins in the Dinaledi Chamber, Cradle of Humankind, South Africa. Journal of Human Evolution 96, 145–148.

Von Mirbach, J. 2015. *Homo naledi*: Scientific sensation or just a big show? DW.com, http://dw.com/p/1GVtx (accessed 14 September 2015).

White, T.D., Asfaw, B., DeGusta, D., Gilbert, H., Richards, G.D., Suwa, G., Howell, F.C., Pleistocene *Homo sapiens* from Middle Awash, Ethiopia. Nature 423, 742–747.

Wiens, J.J., 1995. Polymorphic characters in phylogenetic systematics. Systematic Biology 44, 482–500.

Wiens, J.J., 2001. Character analysis in morphological phylogenetics: problems and solutions. Systematic Biology 50, 689–699.

Williams, S., García-Martínez, D., Bastir, M., Meyer, M.R., Nalla, S., Hawks, J., Schid, P., Churchill, S.E., Berger, L.R., 2017. The vertebrae and ribs of *Homo naledi.* Journal of Human Evolution 104, 136–154.

Wood, B., Abbott, S., 1983. Analysis of the dental morphology of Plio-Pleistocene hominids. I. Mandibular molars: crown area measurements and morphological traits. Journal of Anatomy 136, 197–219.

Wood, B., Engleman, C., 1988. Analysis of the dental morphology of Plio-Pleistocene hominids. V. Maxillary postcanine tooth morphology. Journal of Anatomy 161, 1–35.

Zanolli, C., Mazurier, A., 2013. Endostructural characterization of the *H. heidelbergensis* dental remains from the early Middle Pleistocene site of Tighenif, Algeria. C. R. Palevol 12, 293–304.

Figure legends

Figure 1. Three-dimensional multidimensional scaling of 78-trait mean measure of divergence distances among *Homo naledi* and eight comparative samples. Abbreviations: AFA = *Australopithecus afarensis*; AFR = *Australopithecus africanus*; PBO = *Paranthropus boisei*; PRO = *Paranthropus robustus*; HHA = *Homo habilis*; HER = *Homo erectus*; HNA = *Homo naledi*; EAF = East African Holocene *Homo sapiens*; SAF = South African Holocene *H. sapiens*. See main text for sample details.

Figure 2. Three-dimensional scatterplot of the first three principal components among *Homo naledi* and eight comparative samples for 57 dental traits (Table 3). It accounts for 68.05% of the total variance (37.67% on Dimension 1, 18.43% on Dimension 2, and 11.95% on Dimension 3). See abbreviations defined in Table 1 and Figure 1 caption.

Figure 3. Three-dimensional multidimensional scaling of 45-trait mean measure of divergence distances among *Homo naledi* and eight comparative samples. See abbreviations definitions in Table 1 and Figure 1 caption.

Figure 4. Maxillary (A) and mandibular (B) teeth from *Homo naledi* holotype specimen, Dinaledi Hominin 1 (DH1). For this figure 'right' antimeres that follow the order of trait descriptions in the text were created by flipping the left maxilla (U.W. 101-1277) and corresponding left half of the mandible (U.W. 101-1261). The locations of high frequency crown traits in the species are designated by numbers: 1) C^1 double shoveling, 2) C^1 distal accessory ridge, 3) upper molar ASUDAS grade 4–5 metacones, 4) upper molar ASUDAS grade 4–5 hypocones, 5) five principal cusps-only on lower molars, 6) Y-groove pattern-only on lower molars. Locations where crown traits that occur in much lower frequencies than other hominins or are entirely absent are denoted by letters: a = labial curvature I^1; b = tuberculum dentale C^1; c = accessory cusps P^3/P^4; d = buccal median ridge P^4; e = cusp 5 M^1–M^2; f = metaconid placement P_3; g = multiple P_4 lingual cusps; h = transverse crest P_3–P_4; i = asymmetry P_3–P_4; j = deflecting wrinkle M_1–M_3; k = protostylid M_2–M_3 (though note exceptional grade 7 protostylid on M_3 in this particular specimen). See text for details on these and other high- and low-frequency traits.
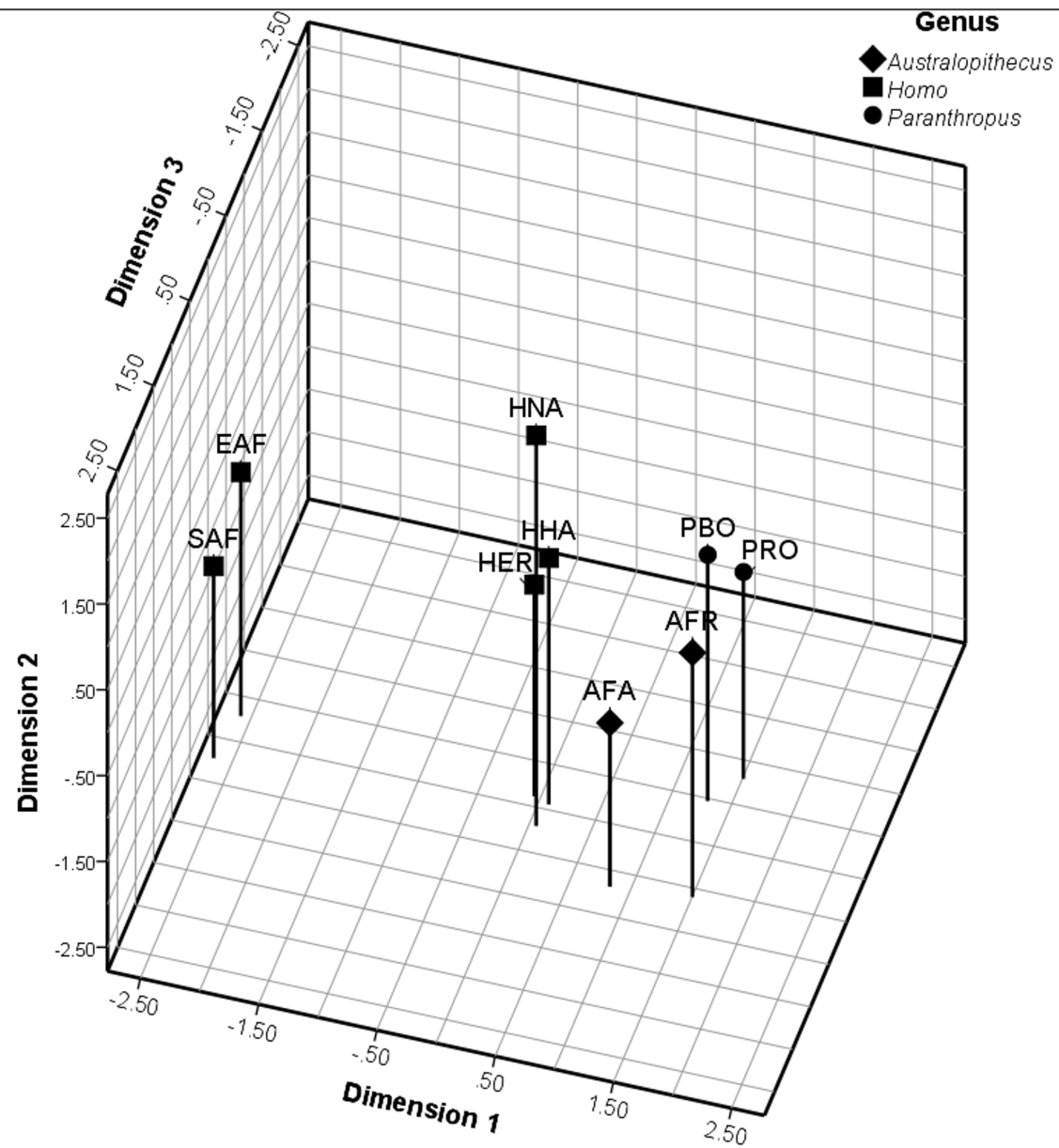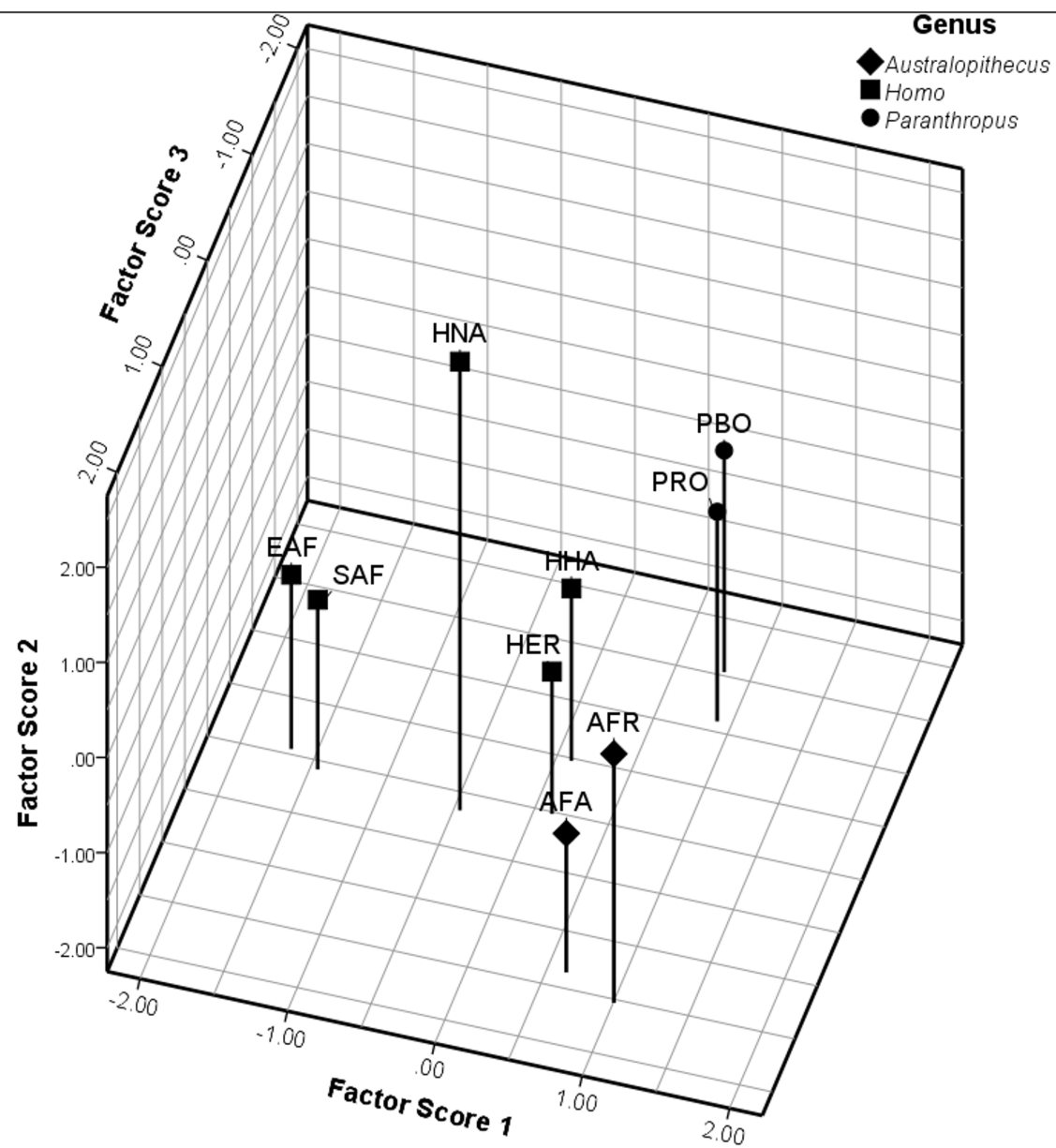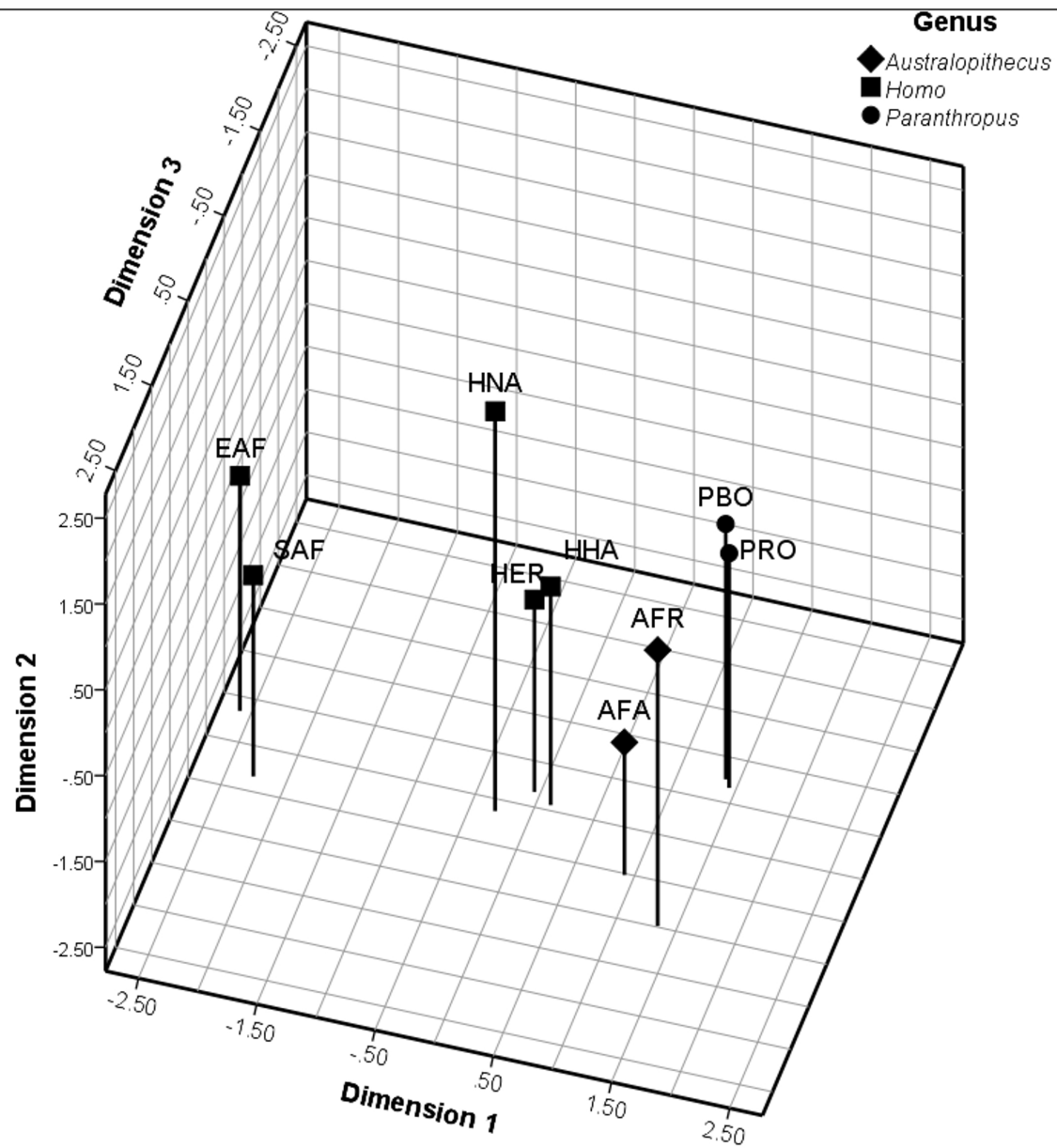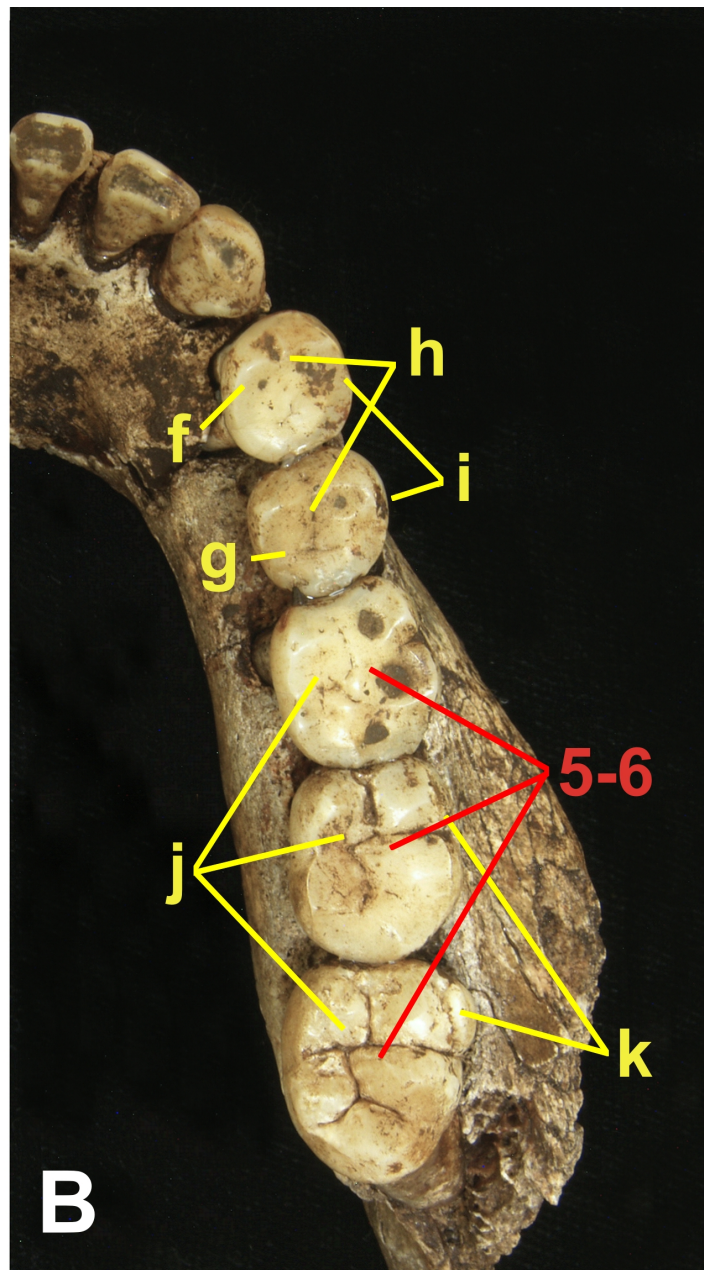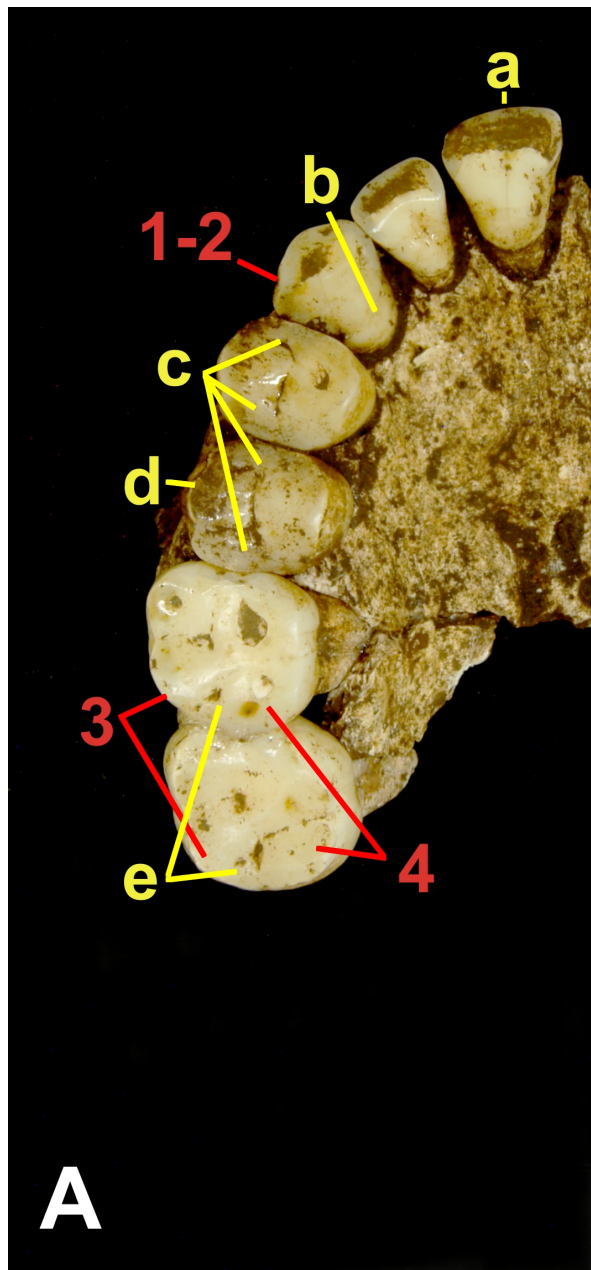
Table 1

Dental trait percentages (%) and number of specimens scored (*n*) for the 11 African hominin samples.

No.	Trait	Sample[a]	AFA	AFR	PBO	PRO	HHA	HER	HMP	HNA	HSE	EAF	SAF
1	Winging I^1 [b]	%	0.00	0.00	0.00	0.00	0.00	0.00	0.00	0.00	100.00	1.37	4.63
	(+=ASU 1)	*n*	4	11	2	21	1	2	1	6	1	73	216
2	Labial curvature I^1	%	55.56	25.00	33.33	66.67	50.00	50.00	100.00	0.00	0.00	10.81	24.59
	(+=ASU 3–4)	*n*	9	12	3	15	2	4	1	4	2	74	122
3	Shoveling I^1	%	0.00	0.00	25.00	7.14	0.00	25.00	0.00	0.00	0.00	0.00	2.60
	(+=ASU 3–6)	*n*	8	10	4	14	2	4	1	4	2	67	77
4	Shoveling I^2	%	0.00	0.00	0.00	12.50	33.33	14.29		0.00	0.00	8.70	14.63
	(+=ASU 3–6)	*n*	6	5	4	8	3	7		6	2	69	82
5	Double shoveling I^1	%	0.00	0.00	0.00	7.14	0.00	0.00	0.00	0.00	0.00	0.00	0.81
	(+=ASU 2–6)	*n*	9	13	4	14	1	4	1	5	1	71	124
6	Double shoveling I^2	%	0.00	0.00	0.00	0.00	0.00	0.00		0.00	0.00	1.43	0.90
	(+=ASU 2–6)	*n*	9	8	4	7	3	7		6	1	70	111
7	Double shoveling C^1	%	0.00	16.67	0.00	0.00	0.00	0.00		36.36		1.19	0.83

#	Trait		1	2	3	4	5	6	7	8	9	10	11
	(+=ASU 2–6)	n	10	12	5	17	2	4		11		84	121
8	Interruption groove I^1	%	0.00	0.00	25.00	0.00	0.00	0.00	0.00	0.00	50.00	0.00	0.00
	(+=ASU 1)	n	7	11	4	14	2	3	1	5	2	62	92
9	Interruption groove I^2	%	0.00	0.00	0.00	0.00	0.00	0.00		0.00	0.00	8.82	2.11
	(+=ASU 1)	n	8	8	4	6	3	7		7	1	68	95
10	Tuberculum dentale I^1	%	42.86	60.00	25.00	42.86	0.00	40.00	100.00	28.57	50.00	6.67	12.82
	(+=ASU 3–6)	n	7	10	4	14	2	5	1	7	2	60	78
11	Tuberculum dentale I^2	%	25.00	14.29	0.00	0.00	0.00	0.00		0.00	0.00	4.41	6.02
	(+=ASU 3–6)	n	8	7	4	7	3	7		7	2	68	83
12	Tuberculum dentale C^1	%	44.44	54.55	50.00	29.41	50.00	50.00		0.00	0.00	32.89	25.33
	(+=ASU 3–6)	n	9	11	4	17	2	4		8	1	76	75
13	Bushman canine C^1	%	0.00	0.00	0.00	0.00	0.00	0.00		0.00	0.00	11.69	42.50
	(+=ASU 1–3)	n	12	13	4	16	3	4		9	1	77	80
14	Distal accessory ridge C^1	%	14.29	0.00	0.00	23.08	0.00	66.67		44.44	0.00	31.34	16.13
	(+=ASU 2–5)	n	7	8	4	13	1	3		9	1	67	62
15	Accessory cusps P^3/P^4	%	44.44	56.25	83.33	83.33	60.00	50.00	0.00	14.29	33.33	31.82	22.99

#	Trait		C1	C2	C3	C4	C5	C6	C7	C8	C9	C10	C11
	(+=ASU 1)	n	9	16	6	24	5	6	3	14	3	88	87
16	Buccal mesial accessory ridge P^3	%	50.00	71.43	50.00	57.14	100.00	60.00	100.00	100.00		11.11	6.25
	(+=ASU 2–4)	n	4	7	4	7	2	5	1	9		9	16
17	Buccal distal accessory ridge P^3	%	66.67	100.00	66.67	100.00	66.67	100.00	100.00	100.00		40.00	30.00
	(+=ASU 2–4)	n	3	5	3	4	3	2	1	9		5	10
18	Buccal mesial accessory ridge P^4	%	100.00	66.67	100.00	45.45	100.00	57.14	100.00	100.00	50.00	60.00	46.15
	(+=ASU 2–4)	n	4	3	2	11	2	7	1	4	2	5	13
19	Buccal distal accessory ridge P^4	%	100.00	100.00	100.00	100.00	100.00	33.33	100.00	100.00	50.00	40.00	60.00
	(+=ASU 2–4)	n	4	3	2	6	2	3	1	3	2	5	10
20	Metacone M^1	%	83.33	85.71	75.00	77.50	72.73	76.92	100.00	61.54	100.00	43.62	43.64
	(+=ASU 5)	n	6	28	8	40	11	13	2	13	2	94	220
21	Metacone M^2	%	25.00	36.67	28.57	19.23	14.29	20.00	0.00	42.86	0.00	7.02	13.72
	(+=ASU 5)	n	4	30	7	26	7	10	3	14	2	114	226
22	Metacone M^3	%	60.00	70.00	66.67	66.67	50.00	100.00	50.00	100.00	75.00	82.41	80.52
	(+=ASU 4–5)	n	5	20	3	21	6	6	4	6	4	108	154
23	Hypocone M^1	%	100.00	100.00	100.00	100.00	100.00	100.00	100.00	100.00	50.00	100.00	98.06

	(+=ASU 4–5)	n	5	28	8	39	11	14	2	13	2	94	206
24	Hypocone M^2	%	100.00	93.13	100.00	96.15	83.33	90.00	50.0	100.00	33.33	52.34	72.36
	(+=ASU 4–5)	n	5	29	7	26	6	10	2	14	3	107	199
25	Hypocone M^3	%	40.00	72.73	75.00	60.87	16.67	60.00	0.00	66.67	25.00	12.62	19.84
	(+=ASU 4–5)	n	5	22	4	23	6	5	4	6	4	103	126
26	Cusp 5 M^1	%	50.00	25.00	14.29	6.67	28.57	36.36	100.00	0.00	0.00	10.81	14.04
	(+=ASU 3–5)	n	6	20	7	30	7	11	1	12	2	74	114
27	Cusp 5 M^2	%	50.00	70.83	50.00	47.62	20.00	22.22	100.00	8.33	50.00	2.06	25.41
	(+=ASU 3–5)	n	2	24	6	21	5	9	1	12	2	97	122
28	Cusp 5 M^3	%	75.00	88.89	33.33	71.43	50.00	40.00	50.00	50.00	50.00	11.58	26.80
	(+=ASU 3–5)	n	4	18	3	21	6	5	2	6	4	95	97
29	Carabelli's cusp M^1	%	50.00	76.47	57.14	20.69	55.56	66.67	0.00	66.67	0.00	32.89	23.68
	(+=ASU 3–7)	n	6	17	7	29	9	9	1	9	1	76	114
30	Carabelli's cusp M^2	%	50.00	85.71	25.00	27.78	50.00	14.29	0.00	33.33	0.00	0.00	3.03
	(+=ASU 3–7)	n	2	21	4	18	6	7	1	12	2	100	132
31	Carabelli's cusp M^3	%	50.00	77.27	33.33	55.00	25.00	0.00	0.00	0.00	0.00	2.02	4.20

	(+=ASU 3–7)	n	6	22	3	20	4	4	4	5	3	99	119
32	Parastyle M^1	%	0.00	0.00	0.00	13.33	0.00	9.09		0.00	0.00	0.00	0.00
	(+=ASU 2–5)	n	3	19	6	30	9	11		14	1	91	153
33	Parastyle M^2	%	33.33	24..0	20.00	4.35	16.67	0.00	0.00	0.00	0.00	0.00	0.00
	(+=ASU 2–5)	n	3	25	5	23	6	5	1	12	1	109	177
34	Parastyle M^3	%	0.00	6.67	0.00	4.76	20.00	0.00	0.00	0.00	0.00	0.00	0.77
	(+=ASU 2–5)	n	2	15	2	21	5	3	2	6	3	100	130
35	Root number P^3	%	0.00	25.00	66.67	60.00	50.00	33.33	100.00	57.14		0.00	0.50
	(+=ASU 3 and above)	n	8	8	3	15	6	3	1	7		49	202
36	Root number P^4	%	100.00	100.00	100.00	92.86	100.00			87.50	0.00	22.50	6.80
	(+=ASU 2 and above)	n	6	4	6	14	2			8	2	40	147
37	Root number M^2	%	100.00	100.00	100.00	100.00	100.00	100.00		100.00		71.70	72.44
	(+=ASU 3 and above)	n	3	6	3	13	2	5		8		53	127
38	Root number M^3	%	80.00	100.00		88.89	100.00	100.00	100.00	100.00	100.00	36.36	16.05
	(+=ASU 3 and above)	n	5	1		9	2	2	1	5	3	33	81
39	Lingual cusp P_3	%	33.33	25.00	60.00	66.67	20.00	12.50	0.00	60.00	50.00	2.73	6.45

	(+=ASU 3–9)	*n*	15	8	5	15	5	8	4	10	2	110	124
40	Lingual cusp P$_4$	%	30.77	41.67	62.50	31.58	25.00	14.29	66.67	0.00	40.00	6.42	1.57
	(+=ASU 8–9)	*n*	13	12	8	19	4	7	3	8	5	109	127
41	Anterior fovea M$_1$	%	50.00	47.06	40.00	60.71	50.00	63.64	100.00	0.00	50.00	21.25	36.67
	(+=ASU 3–4)	*n*	8	17	10	28	4	11	3	10	4	80	90
42	Groove pattern M$_2$	%	86.96	90.91	100.00	100.00	83.33	87.50	66.66	100.00	42.85	65.73	72.08
	(+=ASU Y)	*n*	23	22	15	29	6	16	3	11	7	143	197
43	Groove pattern M$_3$	%	57.14	61.54	70.59	92.86	100.00	88.89	100.00	100.00	20.00	51.72	44.00
	(+=ASU Y)	*n*	7	26	17	28	5	9	3	8	5	116	150
44	Cusp number M$_1$	%	35.71	4.35	61.54	48.28	0.00	15.38	33.33	0.00	12.50	5.22	4.08
	(+=ASU 6 and above)	*n*	14	23	13	29	8	13	3	11	8	115	147
45	Cusp number M$_2$	%	55.00	47.62	90.91	80.77	40.00	57.14	33.33	9.09	28.57	3.91	6.32
	(+=ASU 6 and above)	*n*	20	21	11	26	5	14	3	11	7	128	174
46	Cusp number M$_3$	%	40.00	4.17	58.82	23.08	40.00	22.22	33.33	0.00	0.00	0.00	0.00
	(+=ASU 7 and above)	*n*	10	24	17	26	5	9	3	8	6	121	133
47	Deflecting wrinkle M$_1$	%	12.50	15.00	16.67	15.38	20.00	36.36	0.00	0.00	71.43	5.00	2.06

	(+=ASU 2–3)	n	8	20	12	26	5	11	3	9	7	100	97
48	Deflecting wrinkle M_2	%	33.33	19.05	27.27	36.36	25.00	60.00	0.00	18.18	0.00	0.74	4.49
	(+=ASU 2–3)	n	12	21	11	22	4	10	3	11	6	136	156
49	Deflecting wrinkle M_3	%	42.86	16.67	64.29	50.00	20.00	33.33	0.00	0.00	0.00	6.61	1.50
	(+=ASU 2–3)	n	7	24	14	28	5	9	3	6	4	121	133
50	C1-C2 crest M_1	%	25.00	0.00	0.00	0.00	0.00	0.00	33.33	0.00	0.00	0.97	0.99
	(+=ASU 1)	n	8	20	12	31	5	11	3	10	8	103	101
51	C1-C2 crest M_2	%	0.00	0.00	0.00	0.00	33.33	0.00	0.00	0.00	0.00	0.00	0.59
	(+=ASU 1)	n	14	21	10	24	3	12	3	10	6	134	169
52	C1-C2 crest M_3	%	0.00	0.00	0.00	0.00	0.00	0.00	0.00	0.00	0.00	0.83	0.71
	(+=ASU 1)	n	8	26	16	28	5	10	3	6	5	121	140
53	Protostylid M_1	%	36.36	63.16	14.29	54.17	25.00	23.08	50.00	60.00	33.33	0.00	1.74
	(+=ASU 4–6)	n	11	19	7	24	4	13	2	10	6	116	115
54	Protostylid M_2	%	52.94	75.00	44.44	84.21	50.00	50.00	0.00	40.00	0.00	0.00	2.67
	(+=ASU 4–6)	n	17	20	9	19	4	12	2	10	4	138	150
55	Protostylid M_3	%	83.33	86.36	18.18	68.97	66.67	60.00	100.00	37.50	33.33	2.44	23.40

	(+=ASU 4–6)	*n*	6	22	11	29	6	10	1	8	3	123	141
56	Cusp 7 M$_1$	%	7.14	32.00	0.00	15.63	33.33	53.33	50.00	0.00	85.71	23.77	21.59
	(+=ASU 2–4)	*n*	14	25	16	32	6	15	4	13	7	122	176
57	Cusp 7 M$_2$	%	20.00	47.62	8.33	20.00	14.29	50.00	0.00	0.00	28.57	13.67	9.24
	(+=ASU 2–4)	*n*	15	21	12	25	7	14	3	11	7	139	184
58	Cusp 7 M$_3$	%	55.56	56.52	21.43	41.38	50.00	50.00	33.33	0.00	33.33	10.66	17.81
	(+=ASU 2–4)	*n*	9	23	14	29	6	10	3	7	3	122	146
59	Tomes' Root P$_3$	%	93.33	83.33	100.00	68.42	75.00	62.50	100.00	100.00	0.00	1.96	4.19
	(+=ASU 5)	*n*	15	6	8	19	4	8	1	7	2	51	191
60	Enamel extension-all molars	%	60.00	16.67	20.00	48.48	40.00	17.65	0.00	7.50	10.00	2.44	1.08
	(+=ASU 1)	*n*	15	24	10	33	10	17	10	40	10	123	279
61	Root number P$_3$	%	70.00	80.00	85.71	57.89	66.67	60.00	0.00	100.00	0.00	1.43	1.49
	(+=ASU 2 and above)	*n*	10	5	7	19	3	5	1	6	2	70	201
62	Root number P$_4$	%	80.00	71.43	100.00	77.78	75.00	66.67	0.00	0.00		1.75	0.00
	(+=ASU 2 and above)	*n*	10	7	12	9	4	3	2	2		57	152
63	Root number M$_2$	%	100.00	100.00	100.00	100.00	100.00	100.00	100.00	100.00	100.00	93.44	89.93

	(+=ASU 2 and above)	n	14	4	18	11	6	3	2	2	4	61	149
64	Root number M_3	%	100.00	100.00	100.00	100.00	100.00	100.00	100.00	100.00	100.00	86.36	50.00
	(+=ASU 2 and above)	n	8	1	13	9	5	3	2	4	4	44	72
65	Odontome-all premolars	%	0.00	4.17	8.33	0.00	12.50	0.00	0.00	0.00	0.00	0.00	0.54
	(+=ASU 1)	n	14	24	12	37	8	10	10	33	18	131	186
66	Torsomolar angle M_3	%	10.00	0.00	10.53	0.00	0.00	7.69	0.00	0.00	0.00	11.48	6.84
	(+=ASU 1)	n	10	20	19	24	7	13	2	8	4	122	190
67	Buccal median ridge $P^{3\ c}$	%	25.00	100.00	100.00	100.00	100.00	60.00	0.00	100.00		55.56	27.78
	(+=SEB 2–3)	n	4	5	4	10	3	5	1	8		9	18
68	Buccal median ridge P^4	%	75.00	100.00	100.00	81.82	75.00	85.71	0.00	50.00	100.00	80.00	78.57
	(+=SEB 2–3)	n	4	3	2	11	4	7	1	4	1	5	14
69	Anterior fovea P_3	%	77.78	100.00	75.00	16.67	20.00	80.00	100.00	83.33	100.00	60.00	46.67
	(+=SEB 2–3)	n	18	3	4	6	5	5	2	6	2	5	15
70	Metaconid placement P_3	%	10.53	100.00	100.00	100.00	25.00	20.00	33.33	0.00	50.00	20.00	20.00
	(+=SEB 1)	n	19	4	4	10	4	5	3	7	2	5	15
71	Metaconid height P_3	%	100.00	100.00	100.00	100.00	100.00	50.00	100.00	100.00	100.00	40.00	40.00

	(+=SEB 2–3)	*n*	18	3	4	5	5	4	1	7	2	5	15
72	Transverse crest P_3	%	100.00	0.00	25.00	66.67	100.00	100.00	100.00	0.00	100.00	60.00	81.25
	(+=SEB 1–3)	*n*	16	3	4	6	5	5	3	6	2	5	16
73	Crown asymmetry P_3	%	84.21	100.00	75.00	90.91	0.00	66.67	50.00	0.00	100.00	0.00	0.00
	(+=SEB 2–3)	*n*	19	4	4	11	5	3	2	8	2	5	15
74	Anterior fovea P_4	%	9.09	33.33	0.00	22.22	33.33	80.00	50.00	33.33	0.00	50.00	40.00
	(+=SEB 2–3)	*n*	11	3	4	9	3	5	2	3	5	4	15
75	Metaconid placement P_4	%	71.43	100.00	100.00	100.00	66.67	60.00	100.00	60.00	83.33	50.00	73.33
	(+=SEB 1)	*n*	14	4	5	12	3	5	3	5	6	4	15
76	Metaconid height P_4	%	100.00	100.00	100.00	100.00	100.00	100.00	100.00	100.00	100.00	100.00	100.00
	(+=SEB 2–3)	*n*	14	4	5	12	3	4	1	5	6	4	15
77	Transverse crest P_4	%	100.00	50.00	0.00	16.67	25.00	40.00	75.00	0.00	0.00	25.00	25.00
	(+=SEB 1–3)	*n*	10	4	4	12	4	5	4	3	6	4	16
78	Crown asymmetry P_4	%	0.00	0.00	0.00	16.67	0.00	0.00	50.00	0.00	0.00	0.00	0.00
	(+=SEB 2–3)	*n*	16	4	5	12	4	5	2	5	6	4	17

[a] Abbreviations: AFA = *Australopithecus afarensis*; AFR = *Australopithecus africanus*; PBO = *Paranthropus boisei*; PRO = *Paranthropus robustus*; HHA = *Homo habilis*; HER = *Homo erectus*; HMP = Middle Pleistocene *Homo;* HNA = *Homo naledi*; HSE = Middle and Late Pleistocene (i.e., early) *Homo sapiens*; EAF

= East African Holocene *Homo sapiens*; SAF = South African Holocene *H. sapiens* (see text for sample details).

[b] Arizona State University Dental Anthropology System traits and rank-scale trait breakpoints described in Turner et al. (1991), Irish (1993, 1998), and Scott and Turner (1997), where '+' refers to grade(s) at which trait is considered to be present (see text for dichotomization details).

[c] Premolar traits and rank-scale breakpoints defined and used by S.E.B. (e.g., Bailey, 2002a, b, Bailey and Lynch, 2005; Bailey and Hublin, 2013), where '+' refers to grade(s) at which trait is considered to be present (see text for dichotomization details).

Table 2.

Means measure of divergence (MMD) distance matrix for nine of the 11 hominin samples based on 78 dental traits (see Table 1).

	AFA	AFR	PBO	PRO	HHA	HER	HNA	EAF	SAF
AFA[a]	0	<u>0.083</u>	<u>0.057</u>	0.155	<u>0.000</u> [b]	<u>0.000</u>	**0.407**	0.648	0.637
AFR	<u>0.083</u>	0	<u>0.010</u>	<u>0.058</u>	<u>0.046</u>	0.104	**0.303**	0.791	0.801
PBO	<u>0.057</u>	<u>0.010</u>	0	<u>0.000</u>	<u>0.000</u>	<u>0.060</u>	**0.271**	0.707	0.770
PRO	0.155	<u>0.058</u>	<u>0.000</u>	0	<u>0.004</u>	0.087	**0.407**	0.805	0.814
HHA	<u>0.000</u>	<u>0.046</u>	<u>0.000</u>	<u>0.004</u>	0	<u>0.000</u>	**0.079**	0.364	0.396
HER	<u>0.000</u>	0.104	<u>0.060</u>	0.087	<u>0.000</u>	0	**0.222**	0.327	0.378
HNA	**0.407**	**0.303**	**0.271**	**0.407**	**0.079**	**0.222**	0	**0.537**	**0.625**
EAF	0.648	0.791	0.707	0.805	0.364	0.327	**0.537**	0	<u>0.005</u>
SAF	0.637	0.801	0.770	0.814	0.396	0.378	**0.625**	<u>0.005</u>	0

[a] Abbreviations as in Table 1. HNA intersample distances in bold for ease of reference.

[b] Underlined MMD distances indicate no significant difference at the 0.025 level.

Table 3

Principal component analysis loadings, eigenvalues, and variance explained for 57 traits in the hominin comparative samples.

	Component 1	Component 2	Component 3
Labial Curvature I[1] [a]	**0.594** [b]	**-0.627**	-0.179
Shoveling I[1] [a]	0.306	-0.216	**-0.532**
Shoveling I[2]	-0.217	-0.410	-0.321
Double shoveling C[1] [a]	-0.031	**0.943**	0.312
Tuberculum dentale I[1] [a]	**0.690**	0.126	0.452
Tuberculum dentale I[2] [a]	0.200	-0.274	**0.803**
Tuberculum dentale C[1] [a]	**0.501**	**-0.698**	0.091
Accessory cusps P[3]-P[4] [a]	**0.756**	-0.332	**-0.501**
Buccal mesial accessory ridge P[3]	**0.529**	**0.524**	0.030
Buccal distal accessory ridge P[3] [a]	**0.687**	0.440	0.087
Metacone M[1] [a]	**0.963**	-0.068	0.181
Metacone M[2] [a]	0.499	**0.763**	0.289
Metacone M[3] [a]	**-0.500**	0.422	0.076
Hypocone M[2] [a]	**0.827**	0.353	0.012
Hypocone M[3] [a]	**0.709**	**0.503**	-0.053
Cusp 5 M[1] [a]	0.342	**-0.637**	**0.513**
Cusp 5 M[2] [a]	**0.809**	-0.162	0.230
Cusp 5 M[3] [a]	**0.786**	0.134	0.478
Carabelli's Cusp M[1]	0.423	0.359	0.381
Carabelli's Cusp M[2] [a]	**0.698**	0.190	**0.524**
Carabelli's Cusp M[3] [a]	**0.786**	-0.109	0.278

Parastyle M^1	0.325	-0.185	-0.356
Parastyle M^2 [a]	**0.655**	-0.229	0.378
Root number P^3 [a]	**0.527**	0.479	**-0.653**
Lingual cusp P$_3$ [a]	**0.595**	**0.559**	-0.408
Lingual cusp P$_4$ [a]	**0.803**	-0.187	-0.222
Anterior fovea M$_1$ [a]	**0.566**	**-0.737**	-0.053
Groove pattern M$_2$ [a]	**0.783**	**0.519**	-0.249
Groove pattern M$_3$	0.370	0.416	-0.383
Cusp number M$_1$ [a]	**0.581**	-0.214	**-0.503**
Cusp number M$_2$ [a]	**0.866**	-0.256	-0.377
Cusp number M$_3$ [a]	**0.605**	-0.350	-0.422
Deflecting wrinkle M$_1$ [a]	**0.518**	-0.489	-0.129
Deflecting wrinkle M$_2$ [a]	**0.626**	-0.229	-0.103
Deflecting wrinkle M$_3$ [a]	**0.736**	-0.342	-0.431
Protostylid M$_1$ [a]	**0.634**	**0.581**	0.329
Protostylid M$_2$	**0.928**	0.102	0.046
Protostylid M$_3$ [a]	**0.724**	-0.123	**0.504**
Cusp 7 M$_1$ [a]	-0.074	**-0.501**	0.196
Cusp 7 M$_2$	0.410	-0.380	0.432
Cusp 7 M$_3$ [a]	**0.667**	**-0.559**	0.362
Tomes' root P$_3$ [a]	**0.815**	0.416	0.027
Enamel extension-all molars [a]	**0.665**	-0.332	0.035
Root number P$_3$	**0.757**	**0.537**	0.031
Root number P$_4$ [a]	**0.896**	-0.364	-0.171
Odontome-all premolars	0.310	-0.096	-0.333

Torsomolar angle M₃ [a]	-0.324	**-0.511**	-0.059
Buccal median ridge P³ [a]	0.487	**0.544**	-0.409
Buccal median ridge P⁴ [a]	0.426	**-0.525**	-0.094
Anterior fovea P₃ [a]	0.136	0.303	**0.570**
Metaconid placement P₃	**0.649**	-0.036	-0.311
Metaconid height P₃ [a]	**0.794**	0.398	-0.012
Transverse crest P₃ [a]	-0.157	**-0.791**	-0.053
Crown asymmetry P₃	**0.849**	-0.218	0.152
Anterior fovea P₄	-0.453	-0.152	0.166
Metaconid placement P₄ [a]	**0.733**	0.013	-0.192
Transverse crest P₄ [a]	0.236	**-0.510**	**0.754**
Eigenvalue	21.470	10.507	6.813
Variance (%)	37.666	18.434	11.953
Total Variance	37.666	56.100	68.053

[a] Denotes the 45 traits used in the final mean measure of divergence comparison (see text for details).

[b] Values in bold indicate strong loadings ($>|0.5|$) as detailed in text.

Table 4

Mean measure of divergence (MMD) distance matrix for nine of the 11 hominin samples based on 45 dental traits.

	AFA	AFR	PBO	PRO	HHA	HER	HNA	EAF	SAF
AFA[a]	0	0.193	0.212	0.210	0.000[b]	0.056	**0.690**	0.842	0.689
AFR	0.193	0	0.186	0.174	0.108	0.230	**0.361**	0.967	0.853
PBO	0.212	0.186	0	0.000	0.013	0.137	**0.416**	0.912	0.883
PRO	0.210	0.174	0.000	0	0.000	0.130	**0.474**	0.956	0.835
HHA	0.000	0.108	0.013	0.000	0	0.000	**0.329**	0.438	0.371
HER	0.056	0.230	0.137	0.130	0.000	0	**0.401**	0.428	0.346
HNA	**0.690**	**0.361**	**0.416**	**0.474**	**0.329**	**0.401**	0	**0.591**	**0.586**
EAF	0.842	0.967	0.912	0.956	0.438	0.428	**0.591**	0	0.011
SAF	0.689	0.853	0.883	0.835	0.371	0.346	**0.586**	0.011	0

[a] Abbreviations as in Table 1. HNA intersample distances in bold for ease of reference.

[b] Underlined MMD distances indicate no significant difference at the 0.025 level.

Supplementary Online Material (SOM)

Ancient teeth, phenetic affinities, and African hominins: Another look at where *Homo naledi* fits in

Joel D. Irish[a,b,*], Shara E. Bailey[c], Debbie Guatelli–Steinberg[d], Lucas K. Delezene[b,e], Lee R. Berger[b]

[a] *Research Centre in Evolutionary Anthropology and Palaeoecology, School of Natural Sciences and Psychology, Liverpool John Moores University, Liverpool L3 3AF UK*

[b] *Evolutionary Studies Institute and Centre for Excellence in PaleoSciences, University of the Witwatersrand, Private Bag 3, WITS 2050, Johannesburg, South Africa*

[c] *Department of Anthropology, New York University, New York, NY 10003, USA*

[d] *Department of Anthropology, Ohio State University, Columbus, OH 43210, USA*

[e] *Department of Anthropology, University of Arkansas, Fayetteville, AR 72701 USA*

* Corresponding author.

E–mail address: J.D.Irish@ljmu.ac.uk (J.D. Irish)

SOM S1

Mean measure of divergence comparison of all African samples, including Middle Pleistocene Homo *and Middle/Late Pleistocene* Homo sapiens

As noted in the published paper, the small heterogeneous African Middle Pleistocene *Homo* (HMP; n = 13 specimens) and Middle/Late Pleistocene *Homo sapiens* (HSE; n = 38) samples, which are closest in age to *Homo naledi* at 335–236 ka (Dirks et al., 2017), have many missing data. Indeed, of the 62 non-missing traits in common across all of the species (i.e., trait numbers 1-3, 5, 8, 10, 15, 18-31, 33-35, 38-61, 63-66, 68-78 in Table 1 of paper), 25 comprise one observation and 33 just two observations in these two comparative samples combined. This issue makes their analysis with the mean measure of divergence distance statistic (MMD), and its recommended minimum sample size (Sjøvold, 1977; Irish, 2010), particularly problematic and any results questionable. That said, because the MMD has proven to be a robust statistic (Irish, 2010), as apparently supported by the 78-trait results, MMD affinities among all African samples are provided here to attempt some quantification of interspecific affinities; this and the following SOM MMD analyses were also requested by two JHE reviewers. The resulting 62-trait phenetic distances are of particular interest between *H. naledi* and the other two Middle/Late Pleistocene samples. However, these data limitations oblige us to focus on qualitative comparisons for the latter in the published paper.

The symmetric MMD matrix is provided in SOM Table S1. Some improbably low MMD values (e.g., HMP with *Australopithecus afarensis*) and many others exhibiting no significant difference despite high intersample values (e.g., HSE with *Paranthropus boisei*) are likely indicative of small sample sizes and concomitant high standard deviations (as detailed in the paper). Other low MMD distances seem more plausible, including HMP with all other Plio-Pleistocene *Homo* samples except *H. naledi*, and HSE showing the closest affinity to EA and SA *H. sapiens* of all fossil samples. The remaining MMD affinities are concordant with those based on all 78 traits (compare SOM Table S1 with Table 2). The subsequent MDS solution provides a good representation of the matrix (SOM Fig. S1), with a Kruskal's stress formula 1 of 0.147 and r^2 of 0.911 (Borgatti, 1997). Intersample patterning is also concordant with that based on 78 traits (compare SOM Fig. S1 and Fig. 2 in the paper), albeit with the plotting of HMP and HSE in the grouping of fossil *Homo* species. To better illustrate the latter affinities, an additional MDS solution for just the seven *Homo* samples (stress = 0.104; r^2 = 0.952) yielded the plot in SOM Figure S2; among other patterning, the

distinctiveness of *H. naledi* and relationship of HSE to EA and SA *H. sapiens* is now more apparent.

SOM S2

Middle Pleistocene comparative material

The deficiency of comparative dental specimens of similar age to the *Homo naledi* material, 335–236 ka (Dirks et al., 2017), leaves the heterogeneous African Middle Pleistocene *Homo* and Middle/Late Pleistocene *Homo sapiens* samples in the present study with too few trait data to allow anything but rough, quantitative intersample comparisons (i.e., SOM S1) using the mean measure of divergence (MMD; Sjøvold, 1977; Irish, 2010). Samples of Holocene African *H. sapiens* are available and used in this study, so only the Middle Pleistocene *Homo* sample was considered for supplementation with non-African, yet closely related hominin data like for the present *Homo erectus* sample (i.e., Dmanisi *Homo ergaster*). Given the African focus of the study, only the most geographically proximate regions were considered, but very few data of this kind are available, with exception. Martinón-Torres et al. (2012) used the same Arizona State University Dental Anthropology System (ASUDAS; Scott and Turner, 2017) as the present study, along with a number of similar non-ASUDAS premolar traits (Bailey, 2002) in dentally characterizing the Middle Pleistocene hominins from Sima de los Huesos (SH), other European *Homo heidelbergensis* (HEI), and European Neanderthals (NEA). However, among other issues (e.g., lack of interobserver error analysis), the "highly derived and Neanderthal character of the Sima de los Huesos dentitions" (Martinón-Torres et al., 2012:55) led us to assume these samples are too disparate to relevantly supplement the African data. This assumption is supported by the marked differences in percentages for many of the 50 traits in common between studies (trait numbers 2–4, 10–14, 16–34, 39–45, 47–58, 67–68, 72, 78 in SOM Table S2). Further, an MMD comparison of these data produces large, significantly different distances between SH, HEI[1], and NEA and the five largest *Homo* samples from the present study (SOM Table S3, SOM Fig. S3), including *H. naledi*. Therefore, the present African Middle Pleistocene *Homo* sample was not supplemented and, again, only qualitative trait comparisons with the other samples are stressed in the published paper. Nevertheless, the dental phenetic comparisons with SH, HEI, and NEA are instructive, notably the extreme dissimilarity evident between

---

[1]The sample's very small size necessitates caution in interpretation of its inter-sample comparisons.

these European samples and *H. naledi.* The MDS solution provides excellent representation of the matrix, with a Kruskal's stress formula 1 of 0.079 and r^2 of 0.959 (Borgatti, 1997).

SOM S3

Mean measure of divergence comparison among all African and European Homo *samples*

Lastly, to again attempt some quantification of affinities among all 10 *Homo* samples, including those which are either 1) of insufficient size (HMP, HSE) for a proper analysis or 2) otherwise not directly pertinent (e.g., SH, HEI, NEA) to the objectives of the published paper (see SOM S1 and S2), a final MMD comparison was undertaken here. The analysis is based on 41 traits in common across these samples (trait numbers 2–3, 10, 18–31, 33–34, 39–45, 47–58, 68, 72, 77 in SOM Table S2). The same caveats and cautions discussed above also apply here. The corresponding MMD matrix is presented below (SOM Table S4), and effects of small sample sizes and high standard deviations are evident, particularly for HMP, and to a lesser extent HSE and HEI. Other intersample affinities seem more plausible, including the low, insignificant MMD value between HMP and HEI, among others. The various phenetic affinities are otherwise similar to those in the preceding MMD comparisons. The MDS solution has a Kruskal's stress formula 1 value of 0.116 and r^2 of 0.946), with the 3D MDS plot provided in SOM Figure S4.

SOM References

Bailey, S.E., 2002. Neandertal dental morphology: implications for modern human origins. Ph.D. Dissertation, Arizona State University.

Borgatti, S.P. 1997. Multidimensional Scaling. www.analytictech.com/borgatti/mds.htm.

Dirks, P., Roberts, E.M., Hilbert-Wolf, H., Kramers, J.D., Hawks, J., Dosseto, A., Duval, M., Elliott, E.M., Grün, R., Hellstrom, J., Herries, A.I.R., Joannes-Boyau, R., Placzek, C.J., Robbins, J., Spandler, C., Wiersma, J., Woodhead, J., Berger, L.R.. 2017. The age of *Homo naledi* and associated sediments in the rising star cave, South Africa. eLife 6, e24231.

Irish, J.D., 2010. The mean measure of divergence: Its utility in model–free and model–bound analyses relative to the Mahalanobis D^2 distance for nonmetric traits. American Journal of Human Biology 22, 378–395.

Martinón-Torres, M., Bermúdez de Castro, J.M., Gómez-Robles, A., Prado-Simón, L., Arsuaga, J.L., 2012. Morphological description and comparison of the dental remains from Atapuerca–Sima de los Huesos site (Spain). Journal of Human Evolution 62, 7–58.

Scott, G.R., Irish, J.D. 2017. Human Tooth Crown and Root Morphology: The Arizona State University Dental Anthropology System. Cambridge University Press, Cambridge.

Sjøvold, T., 1977. Non-metrical divergence between skeletal populations: the theoretical foundation and biological importance of C. A. B. Smith's mean measure of divergence. Ossa 4, 1–133.
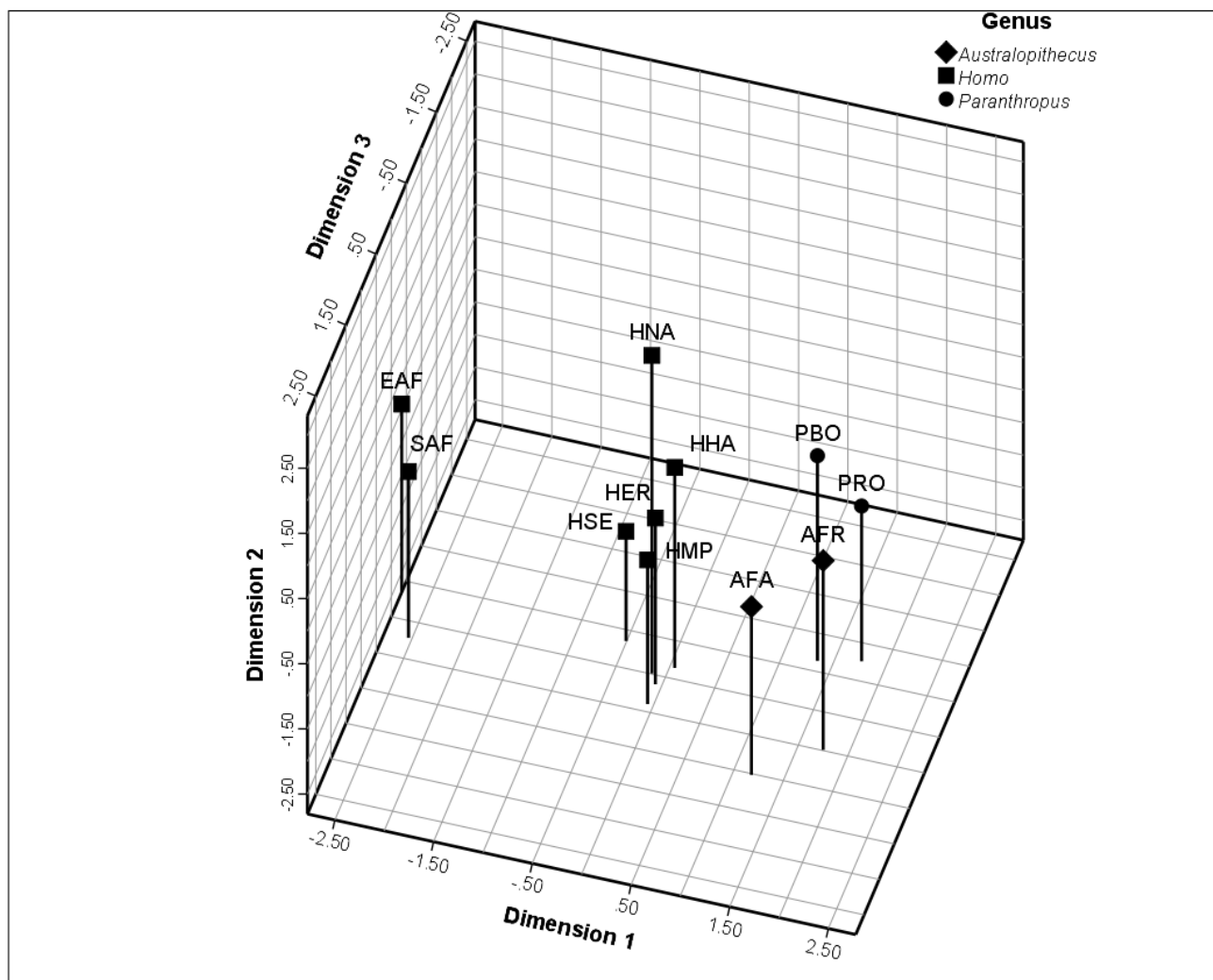
SOM Figure S1. Three-dimensional multidimensional scaling of 62–trait mean measure of divergence distances (from SOM Table S1) among all 11 African hominin samples. See details above in SOM S1. Sample abbreviations listed in SOM Table S1.
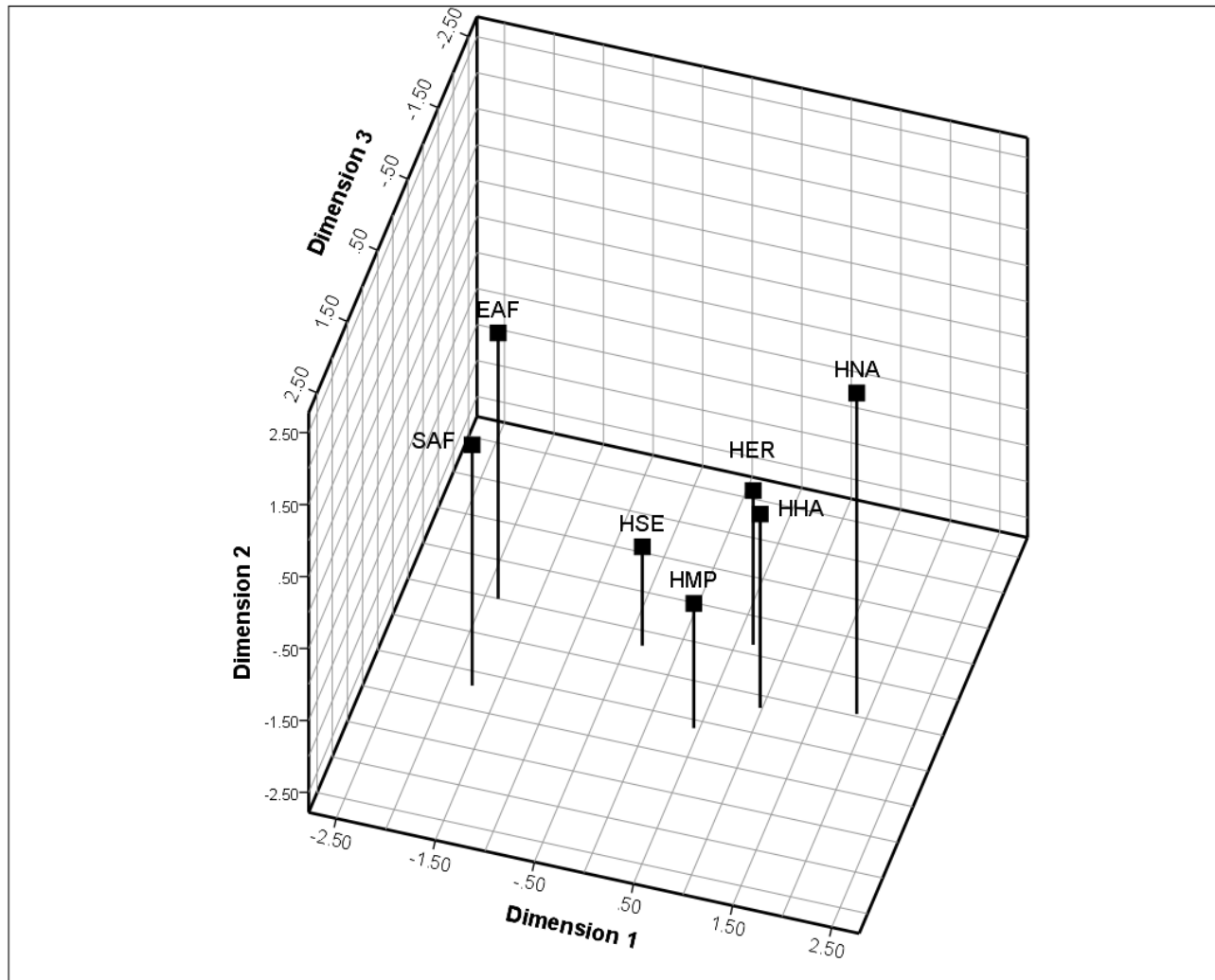
SOM Figure S2. Three-dimensional multidimensional scaling of 62–trait mean measure of divergence distances (from SOM Table S1) among the seven African *Homo* samples. See details above in SOM S1. Sample abbreviations listed in SOM Table S1.
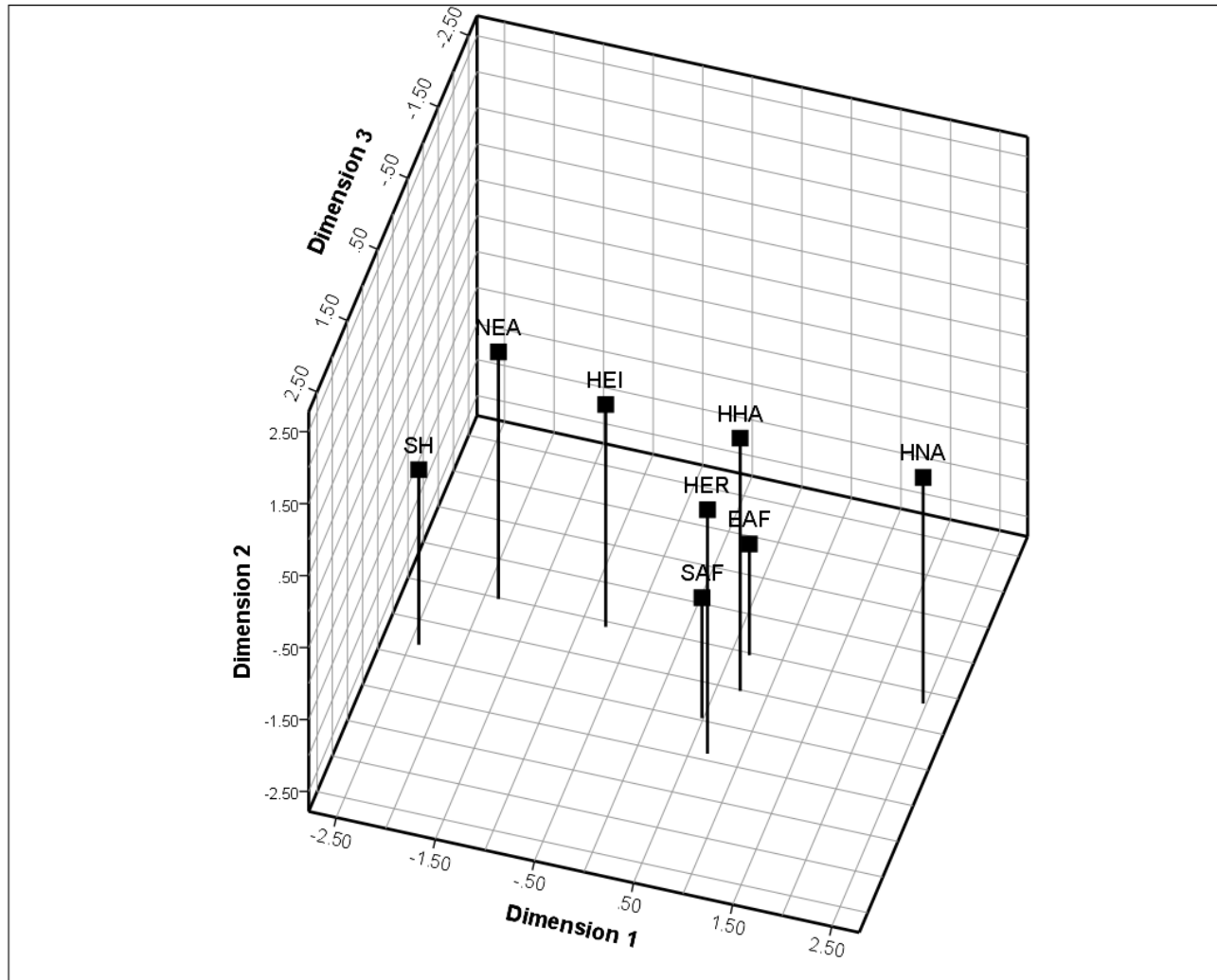
SOM Figure S3. Three-dimensional multidimensional scaling of 50–trait mean measure of divergence distances (from SOM Table S3) among the five largest African *Homo* samples and three European *Homo* samples—with data from Martinón-Torres et al. (2012). See details above in SOM S2. Sample abbreviations listed in SOM Table S2. Note extreme divergence of HNA and to a lesser extent the remaining African *Homo* samples from SH, NEA, and to a lesser extent HEI, as also reflected in the trait percentages (SOM Table S2).

8
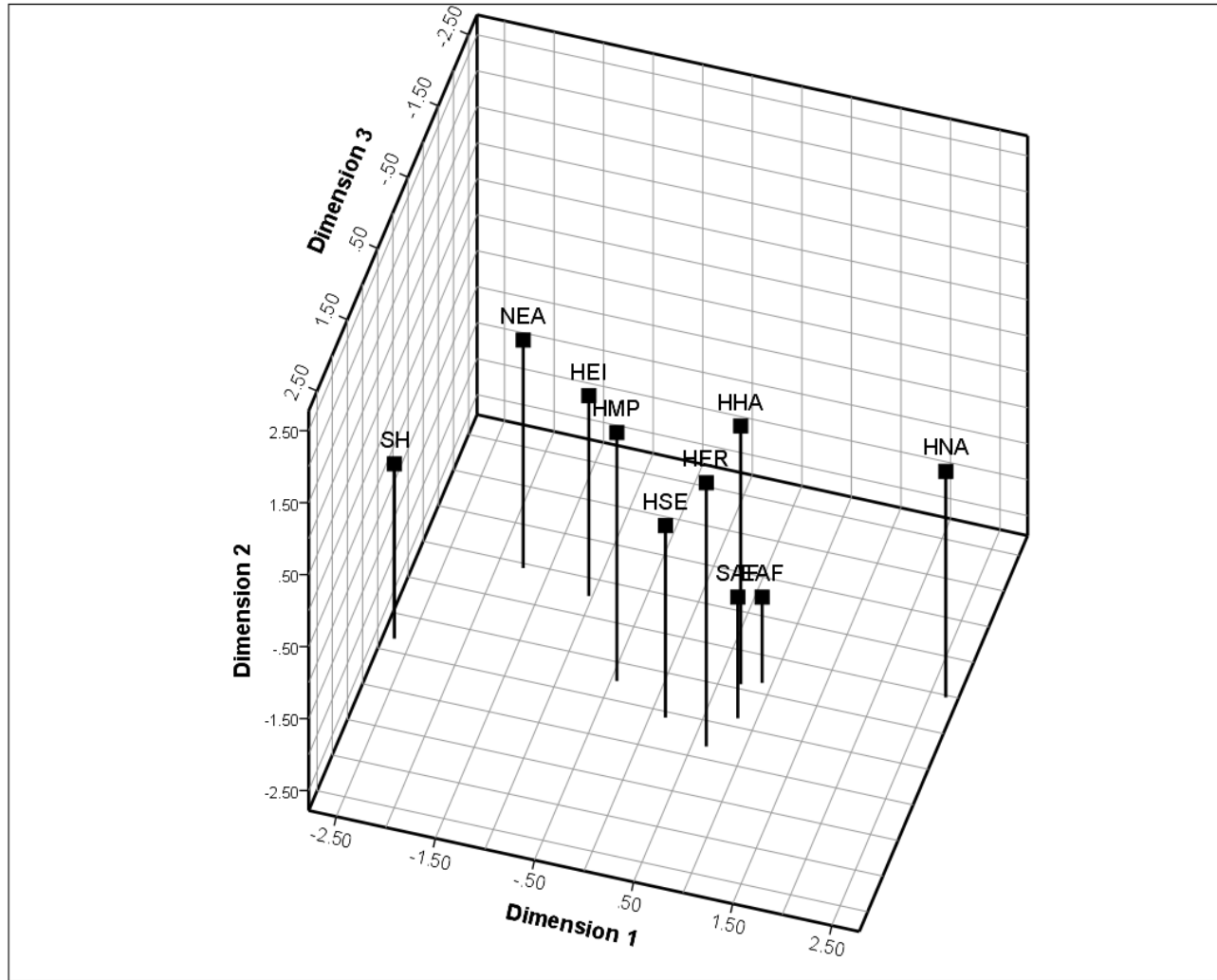
SOM Figure S4. Three-dimensional multidimensional scaling of 41–trait mean measure of divergence distances (from SOM Table S4) among the seven African and three European *Homo* samples. See details in SOM S3. Sample abbreviations listed in SOM Table S2. Again, note the divergence of HNA, but somewhat intermediate location of the small HMP sample between African and European *Homo* groups.

SOM Table S1

Mean measure of divergence (MMD) distance matrix based on 62 dental traits, as discussed above in SOM S1, for all African hominin samples: AFA = *Australopithecus afarensis*; AFR = *Australopithecus africanus*; PBO = *Paranthropus boisei*; PRO = *Paranthropus robustus*; HHA = *Homo habilis*; HER = *Homo erectus*; HMP = Middle Pleistocene *Homo;* HNA = *Homo naledi*; HSE = Middle and Late Pleistocene (i.e., early) *Homo sapiens*; EAF = East African Holocene *Homo sapiens*; SAF = South African Holocene *Homo sapiens.*

	AFA	AFR	PBO	PRO	HHA	HER	HMP	HNA	HSE	EAF	SAF
AFA	0	0.101[a]	0.076	0.155	0.000	0.037	**0.000**[b]	0.380	**0.260**	0.721	0.636
AFR	0.101	0	0.056	0.091	0.129	0.154	**0.145**	0.345	**0.274**	0.827	0.741
PBO	0.076	0.056	0	0.000	0.002	0.110	**0.141**	0.249	**0.216**	0.705	0.689
PRO	0.155	0.091	0.000	0	0.072	0.157	**0.175**	0.475	**0.330**	0.832	0.741
HHA	0.000	0.129	0.002	0.072	0	0.000	**0.000**	0.111	**0.067**	0.347	0.299
HER	0.037	0.154	0.110	0.157	0.000	0	**0.000**	0.264	**0.031**	0.331	0.311
HMP	**0.000**	**0.145**	**0.141**	**0.175**	**0.000**	**0.000**	0	**0.351**	**0.000**	**0.365**	**0.277**
HNA	0.380	0.345	0.249	0.475	0.111	0.264	**0.351**	0	**0.491**	0.485	0.499
HSE	**0.260**	**0.274**	**0.216**	**0.330**	**0.067**	**0.031**	**0.000**	0.491	0	**0.269**	**0.264**
EAF	0.721	0.827	0.705	0.832	0.347	0.331	**0.365**	0.485	**0.269**	0	0.000
SAF	0.636	0.741	0.689	0.741	0.299	0.311	**0.277**	0.499	**0.264**	0.000	0

[a]Underlined MMD distances indicate no significant difference at the 0.025 level.

[b]HMP and HSE intersample distances in bold for ease of reference.

SOM Table S2

Dental trait percentages (%) and number of specimens scored (*n*) for *Homo* samples in current study as discussed above in SOM S2: *Homo habilis* (HHA), *Homo erectus* (HER), African Middle Pleistocene *Homo* (HMP), *Homo naledi* (HNA), Middle and Late Pleistocene (i.e., early) *Homo sapiens* (HSE), East African Holocene *Homo sapiens* (EAF), South African Holocene *Homo sapiens* (SAF), and for Middle Pleistocene Sima de los Huesos *Homo heidelbergensis* (SH), other European *Homo heidelbergensis* (HEI), and European Neanderthal (NEA) derived from Martinón-Torres et al. (2012).

No.	Trait	Sample	HHA	HER	HMP	HNA	HSE	EAF	SAF	SH	HEI	NEA
1	Winging I[1] [a]	%	0.00	0.00	0.00	0.00	100.00	1.37	4.63			
	(+=ASU 1)	*n*	1	2	1	6	1	73	216			
2	Labial curvature I[1]	%	50.00	50.00	100.00	0.00	0.00	10.81	24.59	100.00	100.00	100.00
	(+=ASU 3–5 [b])	*n*	2	4	1	4	2	74	122	20	1	21
3	Shoveling I[1]	%	0.00	25.00	0.00	0.00	0.00	0.00	2.60	90.00	75.00	90.50
	(+=ASU 3–6)	*n*	2	4	1	4	2	67	77	20	4	21
4	Shoveling I[2]	%	33.33	14.29		0.00	0.00	8.70	14.63	100.00	100.00	90.30
	(+=ASU 3–6)	*n*	3	7		6	2	69	82	20	2	31
5	Double shoveling I[1]	%	0.00	0.00	0.00	0.00	0.00	0.00	0.81			
	(+=ASU 2–6)	*n*	1	4	1	5	1	71	124			
6	Double shoveling I[2]	%	0.00	0.00		0.00	0.00	1.43	0.90			
	(+=ASU 2–6)	*n*	3	7		6	1	70	111			
7	Double shoveling C[1]	%	0.00	0.00		36.36		1.19	0.83			
	(+=ASU 2–6)	*n*	2	4		11		84	121			
8	Interruption groove I[1]	%	0.00	0.00	0.00	0.00	50.00	0.00	0.00			
	(+=ASU 1)	*n*	2	3	1	5	2	62	92			

11

#	Trait		1	2	3	4	5	6	7	8	9	10
9	Interruption groove I^2	%	0.00	0.00		0.00	0.00	8.82	2.11			
	(+=ASU 1)	n	3	7		7	1	68	95			
10	Tuberculum dentale I^1	%	0.00	40.00	100.00	28.57	50.00	6.67	12.82	90.00	75.00	90.50
	(+=ASU 3–6)	n	2	5	1	7	2	60	78	20	4	21
11	Tuberculum dentale I^2	%	0.00	0.00		0.00	0.00	4.41	6.02	57.90	0.00	96.70
	(+=ASU 3–6)	n	3	7		7	2	68	83	19	2	30
12	Tuberculum dentale C^1	%	50.00	50.00		0.00	0.00	32.89	25.33	71.50	33.33	100.00
	(+=ASU 3–6)	n	2	4		8	1	76	75	21	3	21
13	Bushman canine C^1	%	0.00	0.00		0.00	0.00	11.69	42.50	94.70	50.00	73.70
	(+=ASU 1–3)	n	3	4		9	1	77	80	19	2	19
14	Distal accessory ridge C^1	%	0.00	66.67		44.44	0.00	31.34	16.13	50.00	50.00	43.70
	(+=ASU 2–5)	n	1	3		9	1	67	62	14	2	16
15	Accessory cusps P^3/P^4	%	60.00	50.00	0.00	14.29	33.33	31.82	22.99			
	(+=ASU 1)	n	5	6	3	14	3	88	87			
16	Buccal mesial accessory ridge P^3	%	100.00	60.00	100.00	100.00		11.11	6.25	0.00	50.00	9.10
	(+=ASU 2–4)	n	2	5	1	9		9	16	14	2	11
17	Buccal distal accessory ridge P^3	%	66.67	100.00	100.00	100.00		40.00	30.00	28.60	50.00	36.40
	(+=ASU 2–4)	n	3	2	1	9		5	10	14	2	11
18	Buccal mesial accessory ridge P^4	%	100.00	57.14	100.00	100.00	50.00	60.00	46.15	46.20	50.00	11.20
	(+=ASU 2–4)	n	2	7	1	4	2	5	13	13	6	9
19	Buccal distal accessory ridge P^4	%	100.00	33.33	100.00	100.00	50.00	40.00	60.00	46.20	80.00	41.70
	(+=ASU 2–4)	n	2	3	1	3	2	5	10	13	5	12

20	Metacone M^1	%	72.73	76.92	100.00	61.54	100.00	43.62	43.64	11.80	0.00	17.40
	(+=ASU 5)	n	11	13	2	13	2	94	220	17	4	23
21	Metacone M^2	%	14.29	20.00	0.00	42.86	0.00	7.02	13.72	0.00	0.00	9.50
	(+=ASU 5)	n	7	10	3	14	2	114	226	18	3	21
22	Metacone M^3	%	50.00	100.00	50.00	100.00	75.00	82.41	80.52	0.00	0.00	16.70
	(+=ASU 4–5)	n	6	6	4	6	4	108	154	21	2	18
23	Hypocone M^1	%	100.00	100.00	100.00	100.00	50.00	100.00	98.06	94.10	100.00	95.70
	(+=ASU 4–5)	n	11	14	2	13	2	94	206	17	5	23
24	Hypocone M^2	%	83.33	90.00	50.0	100.00	33.33	52.34	72.36	16.70	33.33	47.70
	(+=ASU 4–5)	n	6	10	2	14	3	107	199	18	3	21
25	Hypocone M^3	%	16.67	60.00	0.00	66.67	25.00	12.62	19.84	0.00	0.00	0.00
	(+=ASU 4–5)	n	6	5	4	6	4	103	126	21	2	17
26	Cusp 5 M^1	%	28.57	36.36	100.00	0.00	0.00	10.81	14.04	37.50	60.00	31.80
	(+=ASU 3–5)	n	7	11	1	12	2	74	114	16	5	22
27	Cusp 5 M^2	%	20.00	22.22	100.00	8.33	50.00	2.06	25.41	33.40	50.00	25.00
	(+=ASU 3–5)	n	5	9	1	12	2	97	122	18	2	20
28	Cusp 5 M^3	%	50.00	40.00	50.00	50.00	50.00	11.58	26.80	0.00	0.00	41.20
	(+=ASU 3–5)	n	6	5	2	6	4	95	97	21	2	17
29	Carabelli's cusp M^1	%	55.56	66.67	0.00	66.67	0.00	32.89	23.68	0.00	25.00	50.00
	(+=ASU 3–7)	n	9	9	1	9	1	76	114	16	4	20
30	Carabelli's cusp M^2	%	50.00	14.29	0.00	33.33	0.00	0.00	3.03	0.00	50.00	15.80
	(+=ASU 3–7)	n	6	7	1	12	2	100	132	18	2	19

13

#	Trait		C1	C2	C3	C4	C5	C6	C7	C8	C9	C10
31	Carabelli's cusp M^3	%	25.00	0.00	0.00	0.00	0.00	2.02	4.20	14.30	0.00	13.40
	(+=ASU 3–7)	n	4	4	4	5	3	99	119	21	2	15
32	Parastyle M^1	%	0.00	9.09		0.00	0.00	0.00	0.00	0.00	0.00	15.00
	(+=ASU 2–5)	n	9	11		14	1	91	153	17	4	20
33	Parastyle M^2	%	16.67	0.00	0.00	0.00	0.00	0.00	0.00	0.00	0.00	0.00
	(+=ASU 2–5)	n	6	5	1	12	1	109	177	18	3	19
34	Parastyle M^3	%	20.00	0.00	0.00	0.00	0.00	0.00	0.77	4.80	0.00	6.30
	(+=ASU 2–5)	n	5	3	2	6	3	100	130	21	2	16
35	Root number P^3	%	50.00	33.33	100.00	57.14			0.00	0.50		
	(+=ASU 3 and above)	n	6	3	1	7			49	202		
36	Root number P^4	%	100.00			87.50	0.00	22.50	6.80			
	(+=ASU 2 and above)	n	2			8	2	40	147			
37	Root number M^2	%	100.00	100.00		100.00		71.70	72.44			
	(+=ASU 3 and above)	n	2	5		8		53	127			
38	Root number M^3	%	100.00	100.00	100.00	100.00	100.00	36.36	16.05			
	(+=ASU 3 and above)	n	2	2	1	5	3	33	81			
39	Lingual cusp P$_3$	%	20.00	12.50	0.00	60.00	50.00	2.73	6.45	23.50	40.00	55.50
	(+=ASU 3–9)	n	5	8	4	10	2	110	124	17	10	27
40	Lingual cusp P$_4$	%	25.00	14.29	66.67	0.00	40.00	6.42	1.57	95.00	100.00	88.90
	(+=ASU 8–9)	n	4	7	3	8	5	109	127	20	5	27
41	Anterior fovea M$_1$	%	50.00	63.64	100.00	0.00	50.00	21.25	36.67	85.00	57.10	81.30
	(+=ASU 3–4)	n	4	11	3	10	4	80	90	20	7	32

14

42	Groove pattern M$_2$	%	83.33	87.50	66.66	100.00	42.85	65.73	72.08	40.90	55.50	70.80
	(+=ASU Y)	n	6	16	3	11	7	143	197	22	9	24
43	Groove pattern M$_3$	%	100.00	88.89	100.00	100.00	20.00	51.72	44.00	23.50	14.30	60.00
	(+=ASU Y)	n	5	9	3	8	5	116	150	17	7	15
44	Cusp number M$_1$	%	0.00	15.38	33.33	0.00	12.50	5.22	4.08	0.00	16.70	34.50
	(+=ASU 6 and above)	n	8	13	3	11	8	115	147	20	6	29
45	Cusp number M$_2$	%	40.00	57.14	33.33	9.09	28.57	3.91	6.32	42.90	44.40	37.50
	(+=ASU 6 and above)	n	5	14	3	11	7	128	174	21	9	24
46	Cusp number M$_3$	%	40.00	22.22	33.33	0.00	0.00	0.00	0.00			
	(+=ASU 7 and above)	n	5	9	3	8	6	121	133			
47	Deflecting wrinkle M$_1$	%	20.00	36.36	0.00	0.00	71.43	5.00	2.06	10.50	16.70	3.40
	(+=ASU 2–3)	n	5	11	3	9	7	100	97	19	6	29
48	Deflecting wrinkle M$_2$	%	25.00	60.00	0.00	18.18	0.00	0.74	4.49	0.00	22.20	13.00
	(+=ASU 2–3)	n	4	10	3	11	6	136	156	21	9	23
49	Deflecting wrinkle M$_3$	%	20.00	33.33	0.00	0.00	0.00	6.61	1.50	0.00	0.00	0.00
	(+=ASU 2–3)	n	5	9	3	6	4	121	133	22	6	15
50	C1-C2 crest M$_1$	%	0.00	0.00	33.33	0.00	0.00	0.97	0.99	25.00	0.00	14.30
	(+=ASU 1)	n	5	11	3	10	8	103	101	20	6	28
51	C1-C2 crest M$_2$	%	33.33	0.00	0.00	0.00	0.00	0.00	0.59	0.00	11.10	9.10
	(+=ASU 1)	n	3	12	3	10	6	134	169	21	9	22
52	C1-C2 crest M$_3$	%	0.00	0.00	0.00	0.00	0.00	0.83	0.71	56.50	14.30	18.80
	(+=ASU 1)	n	5	10	3	6	5	121	140	23	7	16

#	Trait		1	2	3	4	5	6	7	8	9	10
53	Protostylid M_1	%	25.00	23.08	50.00	60.00	33.33	0.00	1.74	0.00	0.00	0.00
	(+=ASU 4–6)	n	4	13	2	10	6	116	115	21	6	31
54	Protostylid M_2	%	50.00	50.00	0.00	40.00	0.00	0.00	2.67	0.00	0.00	0.00
	(+=ASU 4–6)	n	4	12	2	10	4	138	150	21	9	22
55	Protostylid M_3	%	66.67	60.00	100.00	37.50	33.33	2.44	23.40	9.60	0.00	0.00
	(+=ASU 4–6)	n	6	10	1	8	3	123	141	21	7	13
56	Cusp 7 M_1	%	33.33	53.33	50.00	0.00	85.71	23.77	21.59	35.00	33.40	55.20
	(+=ASU 2–4)	n	6	15	4	13	7	122	176	20	6	29
57	Cusp 7 M_2	%	14.29	50.00	0.00	0.00	28.57	13.67	9.24	55.00	50.00	56.50
	(+=ASU 2–4)	n	7	14	3	11	7	139	184	20	8	23
58	Cusp 7 M_3	%	50.00	50.00	33.33	0.00	33.33	10.66	17.81	79.20	0.00	40.00
	(+=ASU 2–4)	n	6	10	3	7	3	122	146	21	6	15
59	Tomes' Root P_3	%	75.00	62.50	100.00	100.00	0.00	1.96	4.19			
	(+=ASU 5)	n	4	8	1	7	2	51	191			
60	Enamel extension–all molars	%	40.00	17.65	0.00	7.50	10.00	2.44	1.08			
	(+=ASU 1)	n	10	17	10	40	10	123	279			
61	Root number P_3	%	66.67	60.00	0.00	100.00	0.00	1.43	1.49			
	(+=ASU 2 and above)	n	3	5	1	6	2	70	201			
62	Root number P_4	%	75.00	66.67	0.00	0.00		1.75	0.00			
	(+=ASU 2 and above)	n	4	3	2	2		57	152			
63	Root number M_2	%	100.00	100.00	100.00	100.00	100.00	93.44	89.93			
	(+=ASU 2 and above)	n	6	3	2	2	4	61	149			

#	Trait		C1	C2	C3	C4	C5	C6	C7	C8	C9	C10
64	Root number M_3	%	100.00	100.00	100.00	100.00	100.00	86.36	50.00			
	(+=ASU 2 and above)	n	5	3	2	4	4	44	72			
65	Odontome–all premolars	%	12.50	0.00	0.00	0.00	0.00	0.00	0.54			
	(+=ASU 1)	n	8	10	10	33	18	131	186			
66	Torsomolar angle M_3	%	0.00	7.69	0.00	0.00	0.00	11.48	6.84			
	(+=ASU 1)	n	7	13	2	8	4	122	190			
67	Buccal median ridge P^3 [c]	%	100.00	60.00	0.00	100.00		55.56	27.78	29.40	50.00	40.00
	(+=SEB 2–3)	n	3	5	1	8		9	18	17	2	15
68	Buccal median ridge P^4	%	75.00	85.71	0.00	50.00	100.00	80.00	78.57	66.70	50.00	33.33
	(+=SEB 2–3)	n	4	7	1	4	1	5	14	18	6	15
69	Anterior fovea P_3	%	20.00	80.00	100.00	83.33	100.00	60.00	46.67			
	(+=SEB 2–3)	n	5	5	2	6	2	5	15			
70	Metaconid placement P_3	%	25.00	20.00	33.33	0.00	50.00	20.00	20.00			
	(+=SEB 1)	n	4	5	3	7	2	5	15			
71	Metaconid height P_3	%	100.00	50.00	100.00	100.00	100.00	40.00	40.00			
	(+=SEB 2–3)	n	5	4	1	7	2	5	15			
72	Transverse crest P_3	%	100.00	100.00	100.00	0.00	100.00	60.00	81.25	83.30	40.00	53.80
	(+=SEB 1–3)	n	5	5	3	6	2	5	16	18	10	26
73	Crown asymmetry P_3	%	0.00	66.67	50.00	0.00	100.00	0.00	0.00			
	(+=SEB 2–3)	n	5	3	2	8	2	5	15			
74	Anterior fovea P_4	%	33.33	80.00	50.00	33.33	0.00	50.00	40.00			
	(+=SEB 2–3)	n	3	5	2	3	5	4	15			

#	Trait											
75	Metaconid placement P4	%	66.67	60.00	100.00	60.00	83.33	50.00	73.33			
	(+=SEB 1)	n	3	5	3	5	6	4	15			
76	Metaconid height P4	%	100.00	100.00	100.00	100.00	100.00	100.00	100.00			
	(+=SEB 2–3)	n	3	4	1	5	6	4	15			
77	Transverse crest P4	%	25.00	40.00	75.00	0.00	0.00	25.00	25.00	75.00	20.00	69.20
	(+=SEB 1–3)	n	4	5	4	3	6	4	16	20	5	26
78	Crown asymmetry P4	%	0.00	0.00	50.00	0.00	0.00	0.00	0.00			
	(+=SEB 2–3)	n	4	5	2	5	6	4	17			

[a] Arizona State University Dental Anthropology System traits and rank–scale trait breakpoints, where '+' refers to grade(s) at which trait is considered to be present (see text for dichotomization details).

[b] A fifth grade was added to the standard ASUDAS scoring system for this trait in the Martinón-Torres et al. (2012) study to account for extreme labial curvature seen in the European SH and NEA hominins.

[c] Premolar traits and rank-scale breakpoints defined and used by S.E.B., where '+' refers to grade(s) at which trait is considered to be present (see text for dichotomization details).

SOM Table S3

Mean measure of divergence (MMD) distance matrix based on 50 traits as discussed in SOM S2, from SOM Table S2, for the five largest *Homo* samples from the present study, plus three European *Homo* samples with data derived from Martinón-Torres et al. (2012). Sample abbreviations listed in SOM Table S2. Note large significant distances between the three European samples and others, but general similarity among them.

	HHA	HER	HNA	EAF	SAF	SH	HEI	NEA
HHA	0	0.000[a]	0.177	0.329	0.259	**0.869**	**0.200**	**0.680**
HER	0.000	0	0.351	0.352	0.292	**0.926**	**0.331**	**0.687**
HNA	0.177	0.351	0	0.497	0.527	**1.821**	**0.797**	**1.458**
EAF	0.329	0.352	0.497	0	0.024	**0.918**	**0.423**	**0.858**
SAF	0.259	0.292	0.527	0.024	0	**0.802**	**0.366**	**0.767**
SH	**0.869**	**0.926**	**1.821**	**0.918**	**0.802**	0	0.075	**0.169**
HEI	**0.200**	**0.331**	**0.797**	**0.423**	**0.366**	0.075	0	0.039
NEA	**0.680**	**0.687**	**1.458**	**0.858**	**0.767**	**0.169**	0.039	0

[a]Underlined MMD distances indicate no significant difference at the 0.025 level.

[b]European SH, HEI, and NEA intersample distances in bold for ease of reference.

SOM Table S4

Mean measure of divergence (MMD) distance matrix for all 10 African and European *Homo s*amples based on 41 dental traits, as detailed above in SOM S3, from SOM Table S2. Sample abbreviations listed in SOM Table S2.

	HHA	HER	HNA	EAF	SAF	SH	NEA	HEI	HMP	HSE
HHA	0	0.000	0.216	0.365	0.207	0.736	0.524	0.267	0.000	0.000
HER	0.000	0	0.388	0.407	0.261	0.812	0.526	0.404	0.028	0.007
HNA	0.216	0.388	0	0.434	0.365	1.571	1.120	0.789	0.579	0.434
EAF	0.365	0.407	0.434	0	0.022	0.856	0.733	0.478	0.486	0.177
SAF	0.207	0.261	0.365	0.022	0	0.781	0.650	0.411	0.270	0.078
SH	0.736	0.812	1.571	0.856	0.781	0	0.158	0.063	0.277	0.492
NEA	0.524	0.526	1.120	0.733	0.650	0.158	0	0.000	0.179	0.407
HEI	0.267	0.404	0.789	0.478	0.411	0.063	0.000	0	0.060	0.131
HMP	0.000	0.028	0.579	0.486	0.270	0.277	0.179	0.060	0	0.000
HSE	0.000	0.007	0.434	0.177	0.078	0.492	0.407	0.131	0.000	0

[a]Underlined MMD distances indicate no significant difference at the 0.025 level